Science of the Total Environment 951 (2024) 175613

Contents lists available at ScienceDirect

Science of the Total Environment

journal homepage: www.elsevier.com/locate/scitotenv

Accelerating microplastic contamination in ^{210}Pb dated sediment cores from an urbanized coastal lagoon (NW Mexico) since the 1990s

Ana Carolina Ruiz-Fernández [a,*], Libia Hascibe Pérez-Bernal [a], Joan-Albert Sanchez-Cabeza [a], Gladys Valencia-Castañeda [a], Jorge Feliciano Ontiveros-Cuadras [b], Carlos Manuel Alonso-Hernández [c]

[a] Universidad Nacional Autónoma de México, Instituto de Ciencias del Mar y Limnología, Unidad Académica Mazatlán, Sinaloa, Mexico
[b] Universidad Nacional Autónoma de México, Instituto de Ciencias del Mar y Limnología, UAPOC-Ciudad Universitaria, Mexico City, Mexico
[c] IAEA Marine Environment Laboratories, Monaco

HIGHLIGHTS

- Temporal variation of microplastic (MP) was assessed in urban lagoon sediments.
- The MP contamination trends were evaluated using three ^{210}Pb-dated cores.
- MP accrual depends on anthropogenic input, hydrodynamics and sedimentation.
- MP fluxes increased since 1950s and accelerated in 1990s in the three cores.

GRAPHICAL ABSTRACT

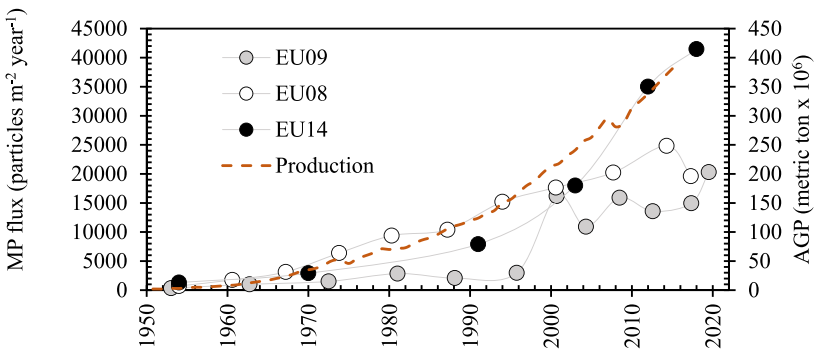

ARTICLE INFO

Editor: Damià Barceló

Keywords:
Inverse estuary
Nile red dye
Sewage treatment plants
Population growth
Gulf of California
Mexican Pacific

ABSTRACT

The ubiquity of microplastics (MP) across all ecosystems raises concerns about their potential harm to the environment and living organisms. Sediments are a MP sink, reflecting long-term accumulation and historical anthropogenic impacts. Three ^{210}Pb-dated sediment cores were used to understand the temporal variations of MP abundances (particles kg^{-1}) and fluxes (particles m^{-2} year^{-1}) within the past century in Estero de Urías Lagoon, an urbanized coastal lagoon in the Mexican Pacific. MP particles, extracted from sediments by density separation (saturated NaCl solution) were counted using a stereomicroscope, under visible and ultraviolet light on Nile red (NR) stained filters. The polymer composition was determined in ~10 % of the suspected MP particles using Fourier Transform Infrared spectrometry. Fibers (66 to 89 % of the total particles) predominated over fragments (11 to 34 %). Before 1950, no MP particles were detected. Polyethylene terephthalate (PET) was the prevalent synthetic polymer (up to 50 % of the particles), while semisynthetic cellulosic fibers were predominant, underscoring the broader scope of anthropogenic contamination. Suspected MP abundances (NR stained filters) were highest in the core collected at the innermost area, which was attributed to the lagoon's hydrodynamics,

* Corresponding author.
E-mail addresses: caro@ola.icmyl.unam.mx (A.C. Ruiz-Fernández), lbernal@ola.icmyl.unam.mx (L.H. Pérez-Bernal), jasanchez@cmarl.unam.mx (J.-A. Sanchez-Cabeza), jontiveros@cmarl.unam.mx (J.F. Ontiveros-Cuadras), C.M.Alonso-Hernandez@iaea.org (C.M. Alonso-Hernández).

https://doi.org/10.1016/j.scitotenv.2024.175613
Received 20 May 2024; Received in revised form 7 August 2024; Accepted 16 August 2024
Available online 19 August 2024

since current velocities decrease from the proximal to the distal area to the sea. From the regression between MP fluxes and time elapsed since sediments deposited, the cores showed consistent accelerated increases of MP burial since mid-20th century, most likely because of the increasing availability of plastic products and population growth, with the consequent increment in plastic waste and wastewater releases. Our findings emphasize the growing MP pollution challenges at EUL, which may directly impact subsistence fishing and shrimp aquaculture activities, threatening local livelihoods and food sources; and also highlight the need for improved waste management and pollution control strategies in rapidly industrializing regions, to protect both aquatic ecosystems and human populations dependent on fishing products.

1. Introduction

Microplastics (MP) are persistent contaminants of global concern owing to their widespread distribution throughout the world's oceans (Chen et al., 2023), their accumulation in bottom sediments (Martin et al., 2022), reaching as far as the deep sea (Pohl et al., 2020); and their capacity to accumulate toxic substances onto the particle's surface (Verla et al., 2019) that may lead to potentially harmful effects on biota (and humans, through the consumption of seafood) because of the ingestion and transfer of MP through trophic levels.

Sediments are the final repository of many long-lived human-produced wastes that reach the surface waters of aquatic ecosystems. Continuous sediment deposition over time creates a chronological archive that allows reconstructing the history of pollutants input, as long as this sedimentary record is reliably dated. The dating method using the natural radionuclide ^{210}Pb ($t_{1/2} = 22.23 \pm 0.12$ years; Bé et al., 2008) is the most widely used for establishing chronologies and reconstructing environmental changes in aquatic ecosystems within the past ~100 to 150 years, a period during which appreciable environmental changes occurred due to population growth and land use changes (Ruiz-Fernández and Hillaire-Marcel, 2009).

The total activity of ^{210}Pb in sediments ($^{210}Pb_{total}$) includes the supported ^{210}Pb fraction ($^{210}Pb_{supported}$) produced in situ within the sediments and the excess ^{210}Pb ($^{210}Pb_{excess}$) fraction, mainly of atmospheric origin, that deposits onto the surface of the sediment column, which is the fraction used for ^{210}Pb dating. The ^{210}Pb-derived chronologies are usually corroborated by using the stratigraphic profiles of the artificial radionuclide ^{137}Cs ($T_{1/2} = 30.05 \pm 0.08$ years; Bé et al., 2006), that was introduced to the environment during atmospheric nuclear tests initiated in 1945 and caused the maximum atmospheric fallout between 1962 and 1964 (UNSCEAR, 2000).

In areas where long-term monitoring programs are scarce or unavailable, ^{210}Pb-dated sediment cores are especially useful because they provide unique environmental records to reconstruct the history of contamination (Ruiz-Fernández and Hillaire-Marcel, 2009). Before the recognition of microplastics as an environmental issue, there were no systematic monitoring programs to evaluate their accumulation in the aquatic environment; thus, the study of ^{210}Pb dated sediment cores is the only reliable method for reconstructing historical MP contamination trends.

Studies elsewhere, using ^{210}Pb-dated sediment cores, have successfully assessed MP contamination in aquatic ecosystems (Matsuguma et al., 2017; Turner et al., 2019; Chen et al., 2020; Dahl et al., 2021) and showed that MP abundances increased over time with increased production, use, and waste generation of plastic. However, current knowledge about burial rates and temporal trends of MP contamination in coastal sediments remains scarce worldwide, mainly due to the analytical challenges posed by both the ^{210}Pb dating of coastal sediments (Barsanti et al., 2020) and the MP analysis (Löder and Gerdts, 2015) in such a complex environmental matrix.

Despite ^{210}Pb is a well-established technique, it is not straight forward (Barsanti et al., 2020). There are still misconceptions about what to expect from a ^{210}Pb profile, such as that recent coastal profiles are often deemed to be mixed and therefore not datable, without considering that atypical ^{210}Pb profiles may be just the result of variations in ^{210}Pb activities owing to sedimentation changes (Sanchez-Cabeza and Ruiz-Fernández, 2012); excess ^{210}Pb activities in low latitudes can be low (Liu et al., 2001) and difficult to detect; there might be difficulties in the robust identification of the ^{210}Pb equilibrium depth (Barsanti et al., 2020); and the corroboration of the ^{210}Pb-derived dates, which is usually done by using ^{137}Cs, is becoming increasingly difficult (Drexler et al., 2018) owing to the low ^{137}Cs activities (often not detectable) resulting from the low fallout in lower latitudes of the northern hemisphere (Aoyama et al., 2006), the time elapsed since the maximum ^{137}Cs fallout (~1963) and the high solubility of ^{137}Cs in seawater (Ruiz-Fernández et al., 2020).

^{210}Pb-dated sedimentary records can provide relevant information on baseline levels that could be used as target values for restoration and to evaluate the evolution and trends (Uddin et al., 2021); to identify the main sources and to elucidate key factors that trigger MP contamination e.g., by contrasting the ^{210}Pb-derived temporal profiles of MP with documental information of known events, such as the starting operations of plastic industry facilities (Alves et al., 2023); and to evaluate whether measures to reduce MP contamination have had the expected effect (Torres and De-la-Torre, 2021). Thus, analyzing MP in ^{210}Pb-dated sediments is relevant to understand when MP began to accumulate and how their sources and fluxes have changed over time, which is essential for developing effective contamination controls and evaluating the efficacity of policies and actions taken to curb ocean plastic pollution at the local, national and global level.

The Estero de Urías Lagoon (EUL) is an urbanized coastal lagoon, in which ^{210}Pb-dated sediments from surrounding saltmarsh areas (Ruiz-Fernández et al., 2009; Ontiveros-Cuadras et al., 2019) showed increasing trace element (e.g., Hg, Ni, Pb and V) contamination trends that were associated with the expansion of urban and industrial activities in Mazatlán City around the lagoon, notably coinciding with the initiation and full operation of a thermoelectric power plant in the 1980s. Subsistence fishing and shrimp aquaculture are still developed at EUL, for which the contribution of MP contamination is undoubtedly an additional environmental concern.

This study, based on the analysis of three ^{210}Pb-dated sediment cores, aimed to assess the levels and the temporal variation of MP abundances and fluxes in EUL since the past century, to reconstruct the historical trends of plastic contamination and explore the factors that might have influenced such trends. We hypothesized that MP abundance and flux have increased from the onset of global plastic commercialization in the 1950s to the present due to the increment in plastic production and population growth. In order to test our hypothesis, we compared the MP fluxes among three periods: <1950 (before mass plastic production), 1950 to <1990 (acceleration of plastic production, Geyer et al., 2017), and 1990–2021 (sampling year). To our knowledge, this is the first historical reconstruction of MP contamination trends based on the analysis of ^{210}Pb-dated sediment cores in Mexico and one of the still few published in the world.

2. Materials and methods

2.1. Study area

EUL, at the entrance of the Gulf of California, is surrounded by the

tourist city of Mazatlán (501,441 inhabitants; INEGI, 2024). The lagoon has a length of ~17 km and a mean depth of 1 to 3 m, except in the navigation channel, in the proximal section of the sea (~3 km), where it is periodically dredged (~2 years) to maintain a depth of ~13 m. Its circulation is dominated by tidal currents, with a speed of 0.91 m s^{-1} in the harbor zone, 0.83 m s^{-1} in the intermediate zone, and 0.31 m s^{-1} in its innermost zone (Cardoso et al., 2015). As rainfall and terrestrial runoff are the only sources of freshwater input into EUL, seasonal weather conditions highly influence its physicochemical characteristics. The prevailing climate is warm sub-humid, with rainfall mostly

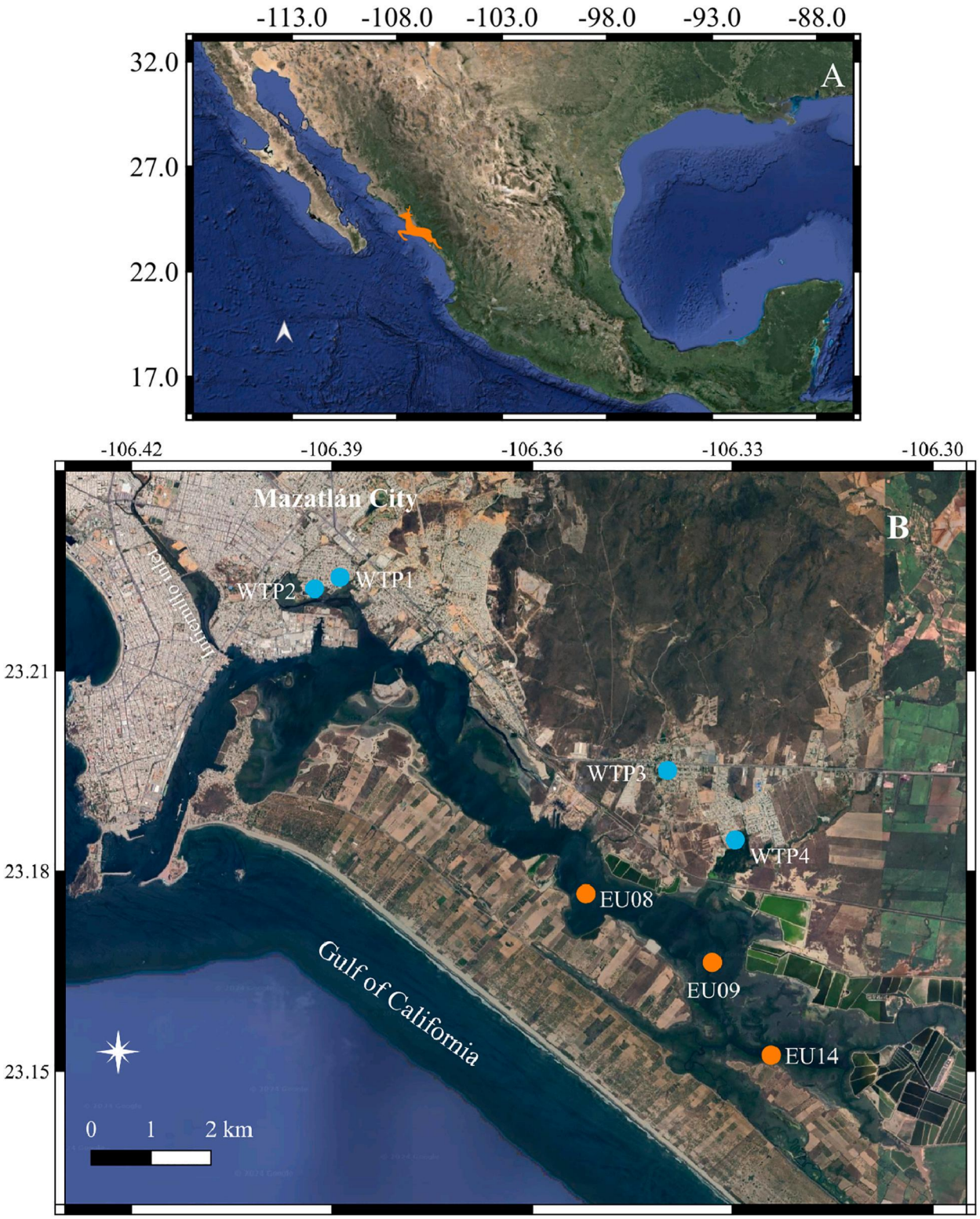

Fig. 1. (A) Location of Mazatlán City (land of deers, in the ancient Nahuatl language); (B) Sampling sites of sediment cores EU08, EU09, and EU14 (orange dots) and location of the wastewater treatment plants WTP1 (Urías 1), WTP2 (Urías 2), WTP3 (Castillo), and WTP4 (Santa Fe) (blue dots) in Estero de Urías Lagoon, Sinaloa, Mexico (southern Gulf of California).

occurring between June and October (mean annual precipitation of 878.7 mm between 1986 and 2016 (INEGI, 2017). In the dry season, the mean value of water temperature is 26.3 °C and of salinity is 39.4 ‰, while during the rainy season, these values increase to 31.5 °C and decrease to 31.7 ‰, respectively. Due to the absence of a continued freshwater supply, EUL exhibits an inverse estuary circulation pattern, leading to water retention and the accumulation of contaminants within the lagoon (Cardoso et al., 2015).

EUL hosts the largest tuna fleet in Latin America, a thermoelectric plant, and it supports commerce, fishing, seafood processing, and naval industry services (Molino-Minero-Re et al., 2014; Ruiz-Fernández et al., 2018). The morphology of EUL has significantly changed since the 1940s due to the growth of Mazatlán City, involving large-scale dredging, the construction of embankments and infrastructure such as roads, docks, navigation channels, breakwaters, shrimp culture facilities, and the urbanization of land reclaimed to the sea through landfill, which have modified the circulation patterns and water mass exchange of the lagoon (Vasavilbazo Saucedo and Covantes Rodríguez, 2012).

Previous studies, performed in ^{210}Pb-dated sediment cores from saltmarsh (Ruiz-Fernández et al., 2016) or mangrove (Aldana-Gutiérrez et al., 2021) areas showed increasing sediment accumulation rates, associated with the extensive land use changes and morphological modifications that EUL has undergone since the middle of last century (Vasavilbazo Saucedo and Covantes Rodríguez, 2012). In addition, the urban and industrial development of Mazatlán City has caused a severe reduction of mangrove surfaces and the contamination of its waters, sediments, and biota with metals and organic pollutants, particularly since the 1980s (Cearreta et al., 2021), promoted by runoff during the rainy season and the discharge of contaminated wastewater into the lagoon.

The lagoon receives effluents from (a) four municipal wastewater treatment plants that consist of primary and secondary treatment (PTARs El Castillo, capacity 8.9 liters per second (L s^{-1}), in operation since 2001; Santa Fe, 48 L s^{-1}, since 2008; Urías I, 400 L s^{-1}, since 2014 and; Urías II, 350 L s^{-1}, since 2021 (CONAGUA, 2022); (b) several shrimp aquaculture production units, mostly surrounding the innermost part of the lagoon, whose residual waters (enriched in particulate residues) are discharged to the lagoon in each harvest period (Fig. 1).

The analysis of MP in suspended and surface sediments of EUL (Rios-Mendoza et al., 2021; Cardoso-Mohedano et al., 2023) indicated that fibers constitute the primary MP form in EUL sediments, with polyethylene and polyethylene terephthalate being the prevalent synthetic polymers. Also, MP fluxes (determined using a sediment trap) are highest during the rainy season, although this seasonal variation is not mirrored in surface sediments, which exhibit consistent MP abundances throughout the year and almost across the whole lagoon, except at the inner zone, where highest abundances are caused by the relatively limited water exchange and proximity to wastewater treatment plants. Despite the poor environmental conditions at EUL, subsistence fishing is still carried out, and the presence of MP threads in the gastrointestinal tracts of 13 fish species from EUL has been reported, from which the polymers identified were polyamide, polyethylene, polypropylene, and polyacrylic (Salazar-Pérez et al., 2021).

2.2. Sampling

The sampling sites were carefully selected to minimize the risk of sediments mixing, avoiding dredged areas (i.e., the navigation channel, Fig. 1) and harbor or anchorage areas for boats (OIEA, 2012, 2021). Sediment cores EU08, EU09, and EU14 (Table 1) were collected, between 2020 and 2021 (Table 1) with a gravity corer Uwitec®, with diver assistance, using a transparent PVC tube (8.6 cm internal diameter and 1-m long). The sediment cores were capped with aluminum foil and transported vertically to the laboratory, where they were extruded and sectioned at 1-cm intervals using a metal spatula (10 cm wide). To prevent contamination of deeper core sections by residues from shallower sections adhering to the inside of the sampling tube, the outer edge of each section was trimmed with a stainless-steel ring slightly smaller in diameter than the tube (OIEA, 2021). The samples were placed in aluminum trays and freeze-dried; dry sediments were ground to fine powder with a porcelain mortar, except aliquots for grain size distribution and MP abundance analysis.

Table 1
Sampling data from sediment cores EU08, EU09, and EU14 collected in Estero de Urías Lagoon, Mexico, at the entrance of the Gulf of California.

Core	Sampling date (dd/mm/yyyy)	Coordinates	Water depth (m)	Length (cm)	Depth (cm), age (years), year AD[a]
EU08	21/08/2020	23.176583° N 106.351967° W	3.3	51	33–34, 111 ± 20, 1909
EU09	21/08/2020	23.166314° N 106.333058° W	1.7	43	27–28, 136 ± 17, 1883
EU14	26/05/2021	23.15243° N 106.32424° W	1.5	40	9–10, 102 ± 20, 1915

[a] According to ^{210}Pb dating, this is the maximum datable depth, age, and year when it was deposited.

2.3. Laboratory analysis

2.3.1. Gamma-ray spectrometry

Activities of total ^{210}Pb ($^{210}Pb_{total}$, 46.5 keV), ^{226}Ra ($^{210}Pb_{supported}$, through ^{214}Pb in secular equilibrium, 351.9 keV), and ^{137}Cs (661.7 keV) were determined by gamma-ray spectrometry (HPGe well-detector, Ortec-Ametek; Díaz-Asencio et al., 2020). Sediment samples were measured for 2 to 3 days to obtain a counting uncertainty <10 % for ^{210}Pb. $^{210}Pb_{excess}$ activities were calculated as the difference between ^{210}Pb and $^{210}Pb_{supported}$.

2.3.2. Loss on ignition

Loss on ignition was determined by combustion in a muffle furnace (Thermo Fisher Scientific BF51800) at 550 °C (LOI_{550}) and at 950 °C (LOI_{950}) to estimate organic matter and carbonate content, respectively (Heiri et al., 2001).

2.3.3. Grain size distribution

The percentages of sand, silt, and clay fractions were determined by laser diffraction using a Malvern Mastersizer 2000E, in sediments previously treated with 30 % H_2O_2 to destroy organic matter.

2.3.4. Microplastic abundance

The suspected MP particles were extracted from the sediment samples (14 sections from the EU08 core, 15 sections from the EU09 core, and 12 sections from the EU14 core) through density separation (Hidalgo-Ruz et al., 2012) using a saturated NaCl solution (density ~ 1.2 g m L^{-1}) and filtration with glass fiber filters, as described in detail in Cardoso-Mohedano et al. (2023). Briefly, 5 g aliquots of dry sediments were treated with H_2O_2 (30 %) to remove organic matter; the remaining sediment was resuspended with a saturated NaCl solution (1.2 ± 0.1 g mL^{-1}), left to settle overnight, and filtered with a vacuum pump (Thermo Barnant 400-3910 Vacuum Pressure Station) using GF/F filters (Whatman glass microfiber filters, 0.7 μm pore size; 4.7 cm diameter). We used 5 g of dry sediment due to the limited sediment mass available in each core section (particularly in the upper, more recent sections with higher water content) since we chose a high-resolution core sectioning approach, with 1 cm thick sections, to achieve good temporal resolution.

The suspected MP particles were counted twice on the total (100 %) surface of the filter; the particles were also classified by color and shape (fragment, film, and fiber; Hidalgo-Ruz et al., 2012) under a LABOMED Luxeo 4Z stereo microscope (35× magnification) using visible light, following the common practice for the analyses of MP in ^{210}Pb-dated sediments, which allowed for global comparison of our results. In

addition, to improve the efficiency of visual inspection, the same filters were stained with a Nile red (NR) solution (Maes et al., 2017) and the suspected particles were counted twice, using a ZEISS Stemi 508 microscope (40× magnification) and a fluorescent lamp NIGHTSEA SFA (light emission 360–380 nm).

To identify the prevailing synthetic polymers in the sediments, twenty particles of each filter were randomly selected using a random number generation function (RAND, Microsoft® Excel® 2019). The particles were transferred one-by-one with a tungsten needle to be analyzed with a Fourier Transform Infrared spectrometer (μFTIR-ATR Thermo Scientific™ Nicolet™ iN™10 MX Ultrafast Imaging Microscope, with germanium microtip ATR) in attenuated total reflection (ATR) mode. Some particles were lost during transfer or broke while being analyzed; however, we ensured to analyze a minimum of 10 % (between 5 and 10 particles) of the suspected MP particles from each filter, accounting for 200 particles among the three cores. To determine the polymer type constituting the particles, the spectra were compared with reference spectra libraries (HR Specta Polymer and Plasticizers by ATR (2008) and Hummel Polymer Sample Library, (1988, 2004, 2008) from Thermo Fisher Scientific Inc.; and "Microplastics_ICML" a homemade library) using the OMNIC™ Specta software. Only polymer matches with a coincidence of ≥75 % were considered valid (Hossain et al., 2020). Approximately 90 % of the particles examined by μFTIR were identified, which suggested the need to improve our reference spectra database.

2.4. Quality control

To minimize cross-contamination, the staff wore cotton clothing and laboratory coats, and the workspaces had limited access to personnel. Sampling equipment was thoroughly washed with concentrated detergent, rinsed with reverse osmosis (RO) water, dried with cotton towels, and stored in wooden transport boxes. The overlying water of the cores was kept until laboratory processing to prevent sediment exposure to air. All working surfaces were cleaned with RO water before use. Materials and samples were kept covered most of the time (with aluminum foil, Petri dishes, or glass watches), except during evaporation or microscopy analyses, and were re-covered during pauses or after finishing analysis.

For MP analyses, quality control included calcination (450 °C, 4 h) of all glassware and glass fiber filters before use to eliminate plastic residues. To avoid sample contamination, water (ultrapure Thermo Scientific™ Barnstead™ Smart2Pure™), H_2O_2, and saline solutions were filtered through a 25 μm mesh sieve. A procedural blank (including all reagents, but not sediment samples, following the same extraction and analysis procedures) was included in every batch of samples, and counting blanks (fiber glass filters within an uncovered petri dish) were also used to quantify airborne contamination during microscopic inspection. A total of 9 procedural blanks and 8 counting blanks were prepared. Suspected MP particles in the blanks were all fibers; they ranged between 3 and 8 items per filter in the procedural blanks (average 6.2 ± 1.5 particles), and from none to 2 particles in the counting blanks (average 1.1 ± 0.6 particles). The number of particles in each procedural blank was subtracted from the suspected MP particle count of the samples in the corresponding analytical batch.

We assessed the method repeatability through the analysis of 2 sets of replicate samples ($n = 6$ each); the coefficients of variation (CV, the percentage ratio of the standard deviation to the mean) were below 10 % (≤8 % for unstained filters and ≤3 % for stained filters) and thus, considered acceptable (Karnes and March, 1993). The mean abundances of MP in both replicates were compared using the Z-score (AMC, 2016), whose values ≤ |2| indicated that the mean abundances were comparable (Z-score = 1.57 for unstained samples and 0.74 for stained samples).

For other analyses performed in the sediments, quality control included the assessment of accuracy through the analysis of reference materials IAEA-300 for ^{210}Pb and ^{137}Cs; and Malvern QAS3002 for grain size; and the assessment of precision by replicate analysis (n = 6). Results obtained from the reference materials were within the reported range of the certified values. The coefficients of variation of the replicate analysis were <8 % for LOI_{550}, and LOI_{950}; and <5 % for ^{210}Pb and grain size.

2.5. Data treatment

2.5.1. ^{210}Pb dating

Age models and mass accumulation rates (MAR, g cm^{-2} year^{-1}) were estimated through the Constant Flux (CF) model (Robbins, 1978). For each sediment layer, the age was calculated using Eq. (1) and the mass accumulation rates using Eq. (2), following the methodology described in Sanchez-Cabeza and Ruiz-Fernández (2012):

$$t(i) = \frac{1}{\lambda} ln \frac{A(0)}{A(i)} \quad (1)$$

$$r(i) = \frac{\lambda\, A(i)}{C(i)} \quad (2)$$

where t(i) (year) is the time elapsed since the sediments at depth i were deposited, r(i) is the mass accumulation rate (g cm^{-2} year^{-1}), C(i) is the $^{210}Pb_{excess}$ activity (Bq kg^{-1}), λ is the ^{210}Pb decay constant (year^{-1}), A(0) is the total inventory of $^{210}Pb_{excess}$ (i.e., the $^{210}Pb_{excess}$ activity accumulated from the core surface down to the equilibrium depth, where $^{210}Pb_{excess}$ is zero), and A(i) is the inventory below the layer to be dated (both in Bq cm^{-2}). The $^{210}Pb_{excess}$ inventories were calculated by integrating over the core length the product of $^{210}Pb_{excess}$ activity (Bq kg^{-1}) and dry mass (kg) divided by the cross-sectional area for each section (cm^{-2}). The radionuclide activities in unmeasured sections were interpolated versus mass depth (g cm^{-2}).

2.5.2. Microplastics

The suspected MP particle abundances (the particle ratio to the sample dry weight) are reported as particles kg^{-1}. The MP flux (particles m^{-2} year^{-1}) is the velocity at which MP particles accumulate per unit area per year, and it was calculated as the product of the suspected MP abundance and MAR at each core section. The slope of the linear regression between MP flux and the elapsed time since sediment deposition (i.e., MP flux/time, particles m^{-2} year^{-2}) is, therefore, the acceleration of the accumulation of suspected MP particles per unit area.

The suspected MP abundances and fluxes were compared among three periods: <1950 (before mass plastic production), 1950 to <1990 (acceleration of plastic production, Geyer et al., 2017), and 1990-2021 (sampling year). Analysis of variance (two-way ANOVA) was used to compare the mean values observed at each period within and among cores. Pearson correlation was used to evaluate the relationship between the suspected MP abundances and the sediment characteristics (i.e., grain size distribution as an indicator of hydrodynamics, and LOI_{550} as an indicator of organic matter content). All analyses were performed at 95 % confidence ($p < 0.05$).

To ascertain whether the color distribution of the suspected MP particles varied based on the sampling site or period, the number of particles (fibers and fragments) per color at each core section was examined using hierarchical cluster analysis (Ward's method, Euclidean distance) with Minitab 15®.

3. Results

3.1. ^{210}Pb dating

In all three sediment cores, ^{210}Pb activity profiles exhibited decreasing activities with depth, though they did not follow the theoretical exponential decay trend (Fig. S1), which was assumed to be

caused by varying sediment inputs with time, as previously observed in other lagoon areas (Ruiz-Fernández et al., 2016; Aldana-Gutiérrez et al., 2021). Based on the age models, all cores contained sediments accumulated >100 years ago (Table 1, Fig. S1). Most ^{137}Cs activities in the three cores were below the minimum detectable activity (MDA; 1.2 Bq kg^{-1}), thus it was not possible to use it for validating the ^{210}Pb-derived age models. MAR values (Fig. S2) were significantly lower ($p < 0.05$) in EU14 (0.03 to 0.13 g cm^{-2} year^{-1}) than those in the other two cores, which were comparable (0.29 to 0.69 g cm^{-2} year^{-1} in EU08; 0.03 to 0.59 g cm^{-2} year^{-1} in EU09).

3.2. Sediment characteristics

The sediments were composed mainly of muddy sands (35–77 % of sand) with similar silt (14–39 %) and clay (7–33 %) percentages (Fig. S2). All cores had comparable clay content, whereas in EU14 the percentage of sand was significantly ($p < 0.05$) higher and of silt significantly lower ($p < 0.05$) than in the other two cores. LOI_{550} (4–8 % in EU08, 4–11 % in EU09, and 7–15 % in EU14) and LOI_{950} (1–3 % in EU08 and 1–2 % in EU09 and EU14) values were comparable among cores (Fig. S2). In core EU08, LOI_{550} percentages decreased towards the core surface as sand percentages increased; whereas in cores EU09 and EU14, LOI_{550} percentages decreased downcore while sand percentages decreased towards the core surface.

3.3. Microplastic abundances and temporal variation

No MP particles were detected in samples before the 1950s with either method. Suspected MP abundances derived from stained filters were significantly ($p < 0.05$) higher, with values ranging from 2 to 10 times greater than those derived from the unstained filters (Fig. 2a,b). The intervals of suspected MP abundances from unstained filters were 400–2120 particle kg^{-1} in EU08, 200–2701 particle kg^{-1} in EU09, and 1196–2278 particle kg^{-1} in EU14, whereas those from stained filters were 201–5604 particle kg^{-1} in EU08, 100–5803 particle kg^{-1} in EU09, and 3296–31,907 particle kg^{-1} in EU14. It was noticeable that, except in EU08, the MP abundances were significantly ($p < 0.05$) correlated with the percentages of LOI_{550} (used as a proxy for organic matter content; $r = 0.95$ in EU09 and 0.93 in EU14) and sand (as indicator of strong hydrodynamic conditions; $r = -0.91$ in EU09 and -0.90 in EU14).

The sediment samples showed a predominance of fibers (mean values were 66 % in EU08, 86 % in EU09, and 89 % in EU14) and, to a lesser extent, fragments (mean values of 34 % in EU08, 14 % in EU09, and 11 % in EU14) ranging in size from 0.1 to 4.3 mm. Blue particles were predominant (mean values of 48 % fibers, 38 % fragments in EU08; 62 % fibers, 70 % fragments in EU09; and 63 % fibers, 74 % fragments in EU14) followed by white/transparent, black, and red particles (Fig. 3). Based on the color of suspected MP particles, cluster analysis categorized the core sections into three main groups (see Fig. S3), among which, group A exclusively contained sections from core EU08, group B included sections from cores EU08 and EU09, and group C comprised all

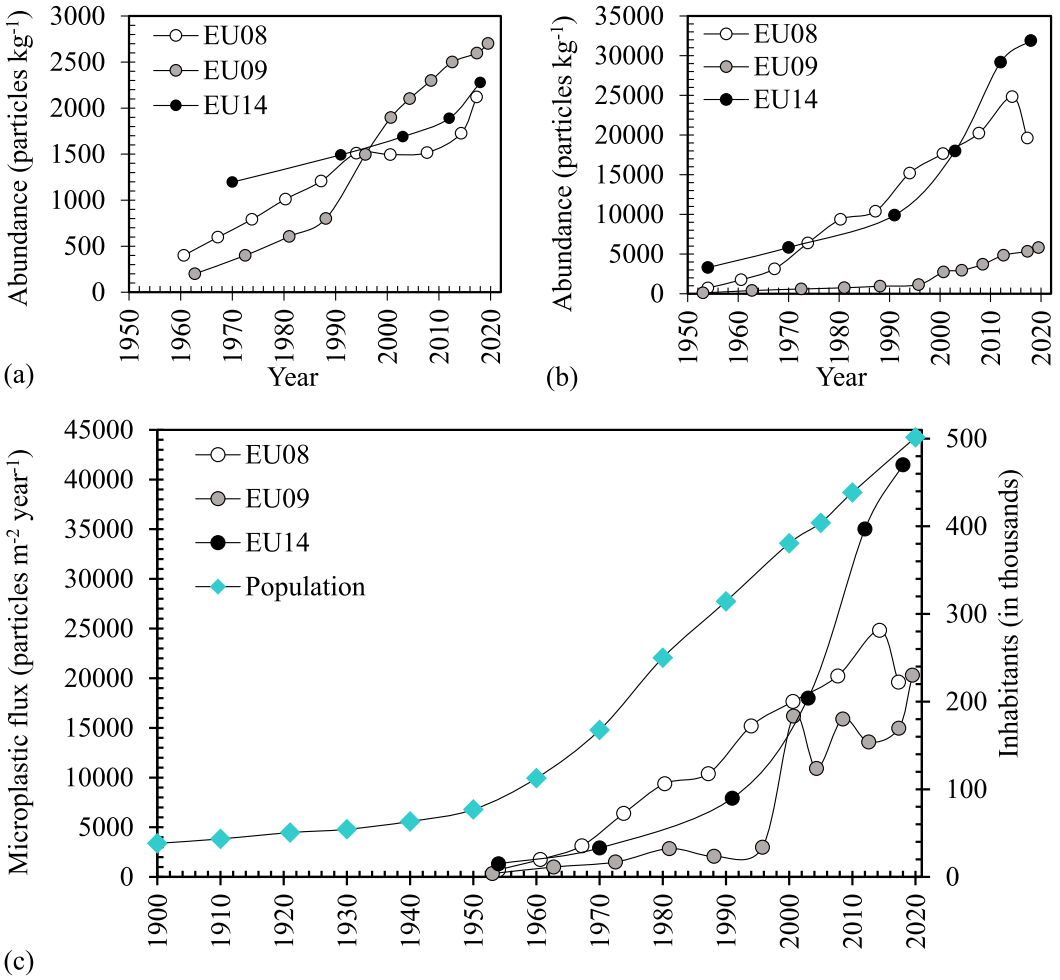

Fig. 2. Temporal variation of microplastic abundance (upper row) and fluxes (lower row) in sediment cores from Estero de Urías Lagoon, México, entrance of the Gulf of California. MP abundances were determined using (a) unstained filters, (b) and (c) Nile red-stained filters.

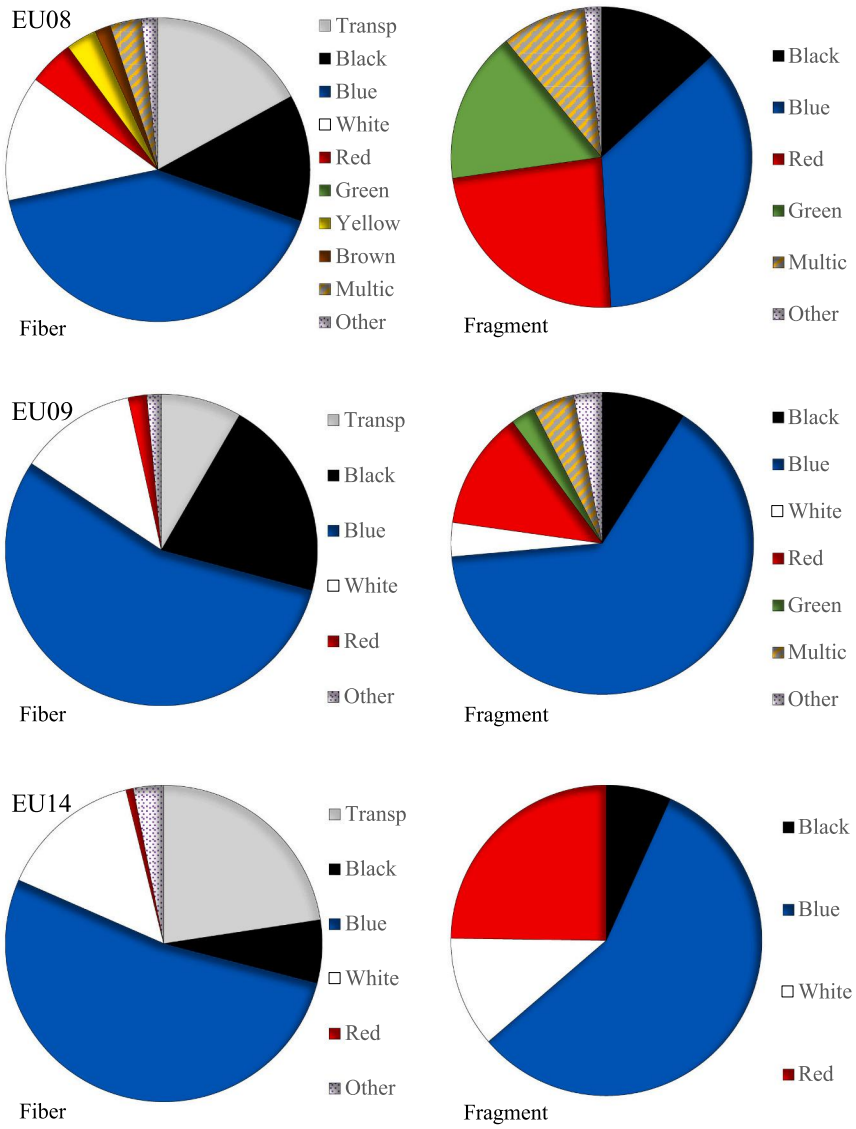

Fig. 3. Mean percentages of color distribution of suspected microplastic particles (fiber and fragment) in sediment cores from Estero de Urías Lagoon, at the Gulf of California entrance.

sections from core EU14 and some from EU09.

A gradual increase in suspected MP abundances was observed since the mid-20th century (Fig. 2a, b). The MP abundances in unstained filters were comparable among the three cores ($p > 0.05$) in both periods (1950 to <1990 and 1990–2021) (Fig. 2a); in contrast, the MP abundances from the stained filters were comparable between EU08 and EU14 for both periods, but significantly higher ($p < 0.5$) than in EU09 (Fig. 2b).

3.4. Microplastic fluxes

The MP fluxes in the three cores, determined from the NR stained filters, were significantly ($p < 0.05$) higher (from 157 % up to 1032 %) than those obtained from unstained filters. Both methods showed that MP fluxes in all cores gradually increased from the 1950s towards the present, with the highest levels recorded during the most recent period (1990–2021). From NR stained filters, the suspected MP fluxes within the early period 1950 to <1990 were comparable between the cores EU09 and EU14, but lower than in EU08, whereas, within the recent period (1990–2021) suspected MP fluxes were comparable between EU08 and EU09, but lower than in EU14 (Fig. 2c).

The slopes of the regression analysis of suspected MP fluxes versus time revealed an accelerated accumulation of suspected MP particles per unit area in all three cores since de 1950s, though this acceleration varied both among cores and across the two periods. In the early period, the descending order among the cores of the acceleration values (annual increase of particles cm^{-2} $year^{1}$) was EU08 (321) > EU14 (100) > EU09 (61), but more recently, this order changed to EU14 (1293) > EU09 (464) > EU08 (293) (Fig. 4).

3.5. Polymer identification of the suspected MP particles

Among the synthetic polymers identified, polyethylene terephthalate (PET) was prevalent, although polyethylene (PE), polypropylene (PP), acrylic (PMMA), and nylon were also occasionally observed (Figs. 5, S4).

Cellulose, rayon, and cellophane were also detected (Fig. S4); however, as their spectra are very similar and commercial libraries may not classify them properly (Cai et al., 2019), they are collectively reported as regenerated cellulosic fibers (RCF, Fig. 5). These were distinguished from natural fibers following Comnea-Stancu et al. (2017) by identifying in the spectra the broad, featureless peaks at 3330 cm^{-1}, the absence of peaks at 1735 cm^{-1}, and the poorly defined peaks at 1105 and 1051

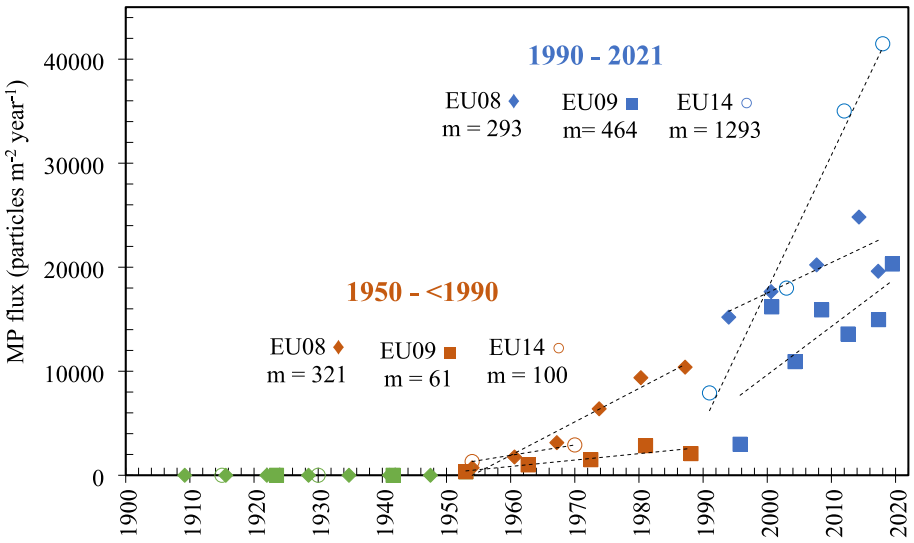

Fig. 4. Regression model of suspected MP fluxes (obtained from the Nile red stained filters) as a function of time (year) since the onset of massive plastic commercialization in the 1950s, from sediment cores collected in Estero de Urías Lagoon, southern Gulf of California. The green dots indicate the null values observed before 1950. The m denotes the slope of each regression model and indicates the annual growth of MP fluxes (i.e., acceleration of MP accumulation).

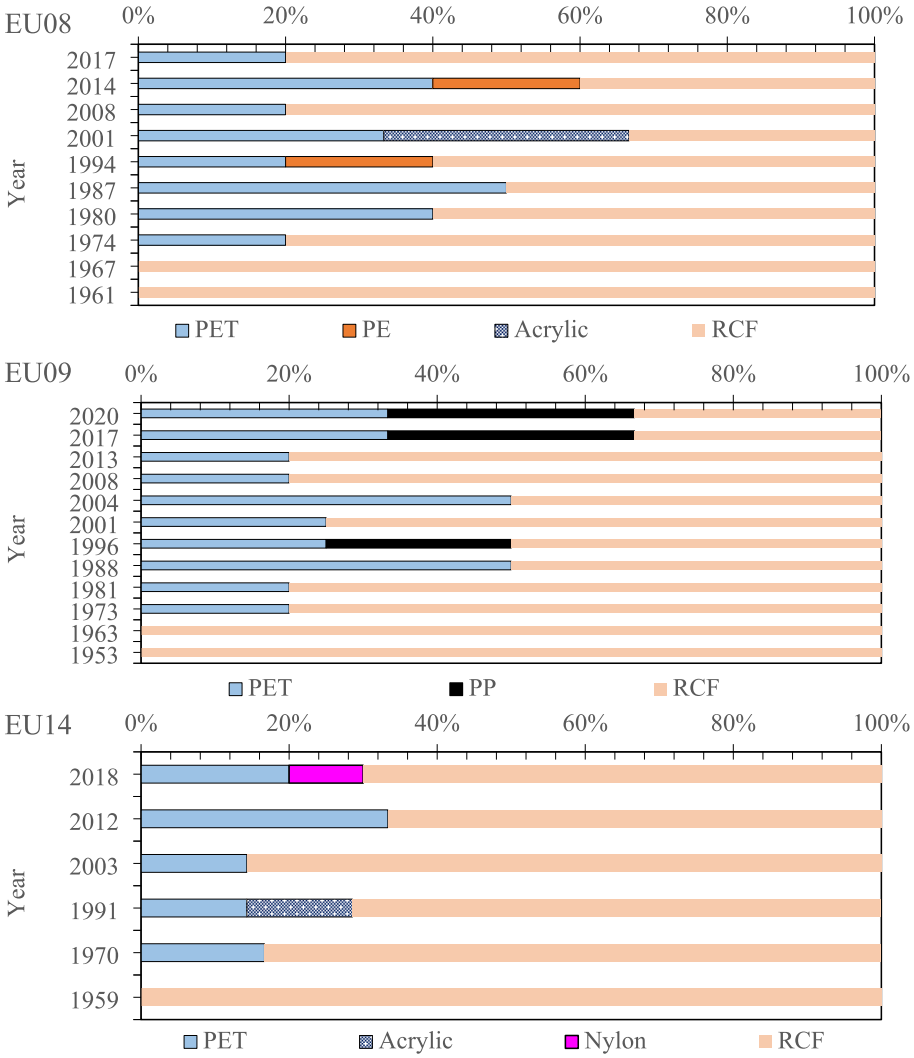

Fig. 5. Type of polymers observed in the sediment cores collected in Estero de Urías Lagoon at the entrance of the Gulf of California. RCP stands for regenerated cellulosic fibers.

cm^{-1} (Fig. S4). These regenerated cellulosic particles were predominant, in some cases, representing up to 100 % of the particles (for example, sediment sections deposited before the 1970s; Fig. 5).

Although cellulose is not a plastic, it is often transformed into man-made products, thus cellulosic particles are considered anthropogenic microdebris, often reported when detected in microplastic studies (Dawson et al., 2023). No corrections or extrapolations of the overall abundances were made based on the results of μFTIR analysis. In our opinion, adjusting the original data without analyzing all particles would be inappropriate.

4. Discussion

4.1. ^{210}Pb dating

All three sediment cores showed non-uniform ^{210}Pb profiles (i.e., deviating from the theoretical profile with activities decreasing with an exponential trend), which could be indicative of post-depositional sediment mixing; however, we assumed that these $^{210}Pb_{excess}$ profiles reflect changes in sediment accumulation rather than mixing because: (a) $^{210}Pb_{excess}$ activities in sediments result from the balance between the $^{210}Pb_{excess}$ flux and sediment input (i.e., mass accumulation rate, MAR; Krishnaswamy et al., 1971; Sanchez-Cabeza and Ruiz-Fernández, 2012) leading to irregular $^{210}Pb_{ex}$ profiles due to sedimentation changes; (b) $^{210}Pb_{excess}$ profiles with regular exponential decline are uncommon since sediment input is influenced by natural factors (e.g., rainfall variability; sporadic storms or hurricanes) and human activities (e.g., dredging, shoreline modifications); (c) previous studies using ^{210}Pb dates cores from saltmarsh (Ruiz-Fernández et al., 2016) and mangrove (Aldana-Gutiérrez et al., 2021) areas of EUL have shown variable sedimentation rates that have been linked to extensive land use changes and morphological modifications that the lagoon has undergone since last century (Vasavilbazo Saucedo and Covantes Rodríguez, 2012); and (d) if the sediment cores were mixed, all variables analyzed in the sediments (including ^{210}Pb, ^{226}Ra, LOI_{550}, LOI_{950}, sand, silt and clay; Figs. S1 and S2) would have shown flat profiles, or at least the same trends, which was not the case.

Sediments on the Mexican Pacific Coast often lack detectable ^{137}Cs activities (Ruiz-Fernández and Hillaire-Marcel, 2009), making it difficult to confirm ^{210}Pb-derived age models. This is attributed to low ^{137}Cs atmospheric fallout in the region during nuclear testing tests (UNSCEAR, 2000), the time elapsed since the maximum global fallout from atmospheric nuclear weapon tests, the high ^{137}Cs solubility in seawater and its potential diagenetic mobility in the sediments (Ruiz-Fernández et al., 2020). Despite ^{137}Cs data was unuseful in corroborating the age models, changes in sand content may serve this purpose at least in cores EU08 and EU09 (Fig. S2). Considering that high hydrodynamic energy levels lead to the accumulation of coarse sediments, while low energy conditions promote the deposition of fine sediments (Alcérreca-Huerta et al., 2022), the higher sand percentages in EU08 and lower ones in EU09 since the 1940s (not visible in EU14; Fig. S2) could be related to the construction of facilities to accommodate deep-draft vessels in the port of Mazatlan in that period (e.g., installation of breakwaters and dredging of the navigation channel; Vasavilbazo Saucedo and Covantes Rodríguez, 2012) as these activities altered the hydrodynamics of the lagoon, increasing current velocities in the area closest to the sea and slowing them down in the inner and shallower parts of the lagoon (Montaño-Ley et al., 2023).

The consistency of MP abundances and flux trends observed among cores and the well-defined onset of the MP record (during the 1950s) is also a reasonable corroboration of ^{210}Pb-derived age models in future studies at EUL, and maybe in other regions worldwide. Other studies elsewhere (Weber and Lechthaler, 2021) have suggested that, due to the widespread distribution of plastics worldwide, their enduring persistence, their clear temporal delimitation, and the lack of a natural background, plastics could serve as a marker of the Anthropocene and for dating young sediments.

4.2. Microplastic contamination

4.2.1. Characteristics of sediments and microplastics

The association between MP and organic matter content in the sediments has been previously explained i) as a result of MP- depositing together with the organic components in the sediments owing to biofouling, since it increases the MP sedimentation (Liu et al., 2023); ii) by the influence of grain size, since finer sediments accumulate more organic carbon, suggesting that finer grains trap more MP particles (Marques Mendes et al., 2021); or iii) due to similarities in densities and sedimentation processes, such as the aggregation of MP with organic matter (e.g., marine snow and fecal pellets of marine organisms) (Maes et al., 2017).

We consider that the significant correlation of MP abundances with the percentages of sand and LOI_{550} in cores EU09 and EU14 reflects the influence of grain size and, thus, the hydrodynamics on sedimentation. Indeed, i) finer particles, including MP, require lower current velocities to settle and accumulate, and ii) sedimentary organic matter tends to concentrate with decreasing grain size and increasing surface area (Horowitz, 1985). Interestingly, these correlations were not observed in core EU08, suggesting that factors other than the sediments' intrinsic characteristics (such as proximity to major sources of contamination or transport processes that homogenize the MP distribution) may also affect MP abundances.

The shape and color of MP particles have been considered important characteristics when addressing MP contamination (Hidalgo-Ruz et al., 2012). Color seems to influence plastic photoaging, microplastic formation, and environmental impacts, since colorants impact the longevity and degradation rate of plastics, with some leading to faster polymer breakdown and microplastic formation (Key et al., 2024). Also, color may lead to preferential uptake of MP by biota (Ugwu et al., 2021) since visual predators may mistake brightly colored MP for prey (Zhao et al., 2022). The predominance of fiber-shaped MP particles and the prevalence of blue color in our study aligns with previous reports elsewhere, which identified blue fibers as the dominant types of MP in marine environments (Athapaththu et al., 2020; Ugwu et al., 2021).

Color of MP has been used to identify MP sources or polymer type; with blue, black, white/transparent, and red reported as the characteristic colors of MP in domestic and industrial wastewater (Deng et al., 2020; Sánchez-Hernández et al., 2021; Stanton et al., 2019); and clear and transparent particles being ascribed to polypropylene, or white to polyethylene, and opaque colors to LDPE (Hidalgo-Ruz et al., 2012). However, plastic weathering can alter both density and color (Duis and Coors, 2016), making color analysis for determining MP type or origin, less significant compared to the more reliable methods of spectral or chemical identification for accurate MP characterization (Zhang et al., 2020).

In our study, the grouping of the sedimentary core sections based on the particle color abundance (Fig. S3) appeared to be associated with the sampling site location, particularly with cores EU08 and EU14 falling into distinct groups (A and C), which could be due to the proximity to predominant MP sources; however, the grouping did not align with deposition periods, suggesting independence from temporal factors. Although the predominant MP source remain unidentified, we speculate that the EU14 sampling site could be more influenced by the discharges from aquaculture facilities, while EU08 and EU09 may be more affected by wastewater treatment plant effluents (Fig. 1). Group B included sections from cores EU08 and EU09, possibly due to current-driven particle homogenization, as previously hinted by Cardoso-Mohedano et al. (2023).

The predominance of fibers agreed with previous observations in suspended (58 to 100 % of all particles) and surface (85–100 %) sediments at EUL (Rios-Mendoza et al., 2021; Cardoso-Mohedano et al., 2023). The presence of fibers is considered an indicator of domestic

effluents (Su et al., 2020) since a large proportion of MP fibers found in the marine environment may have been released from cloth washing (Browne et al., 2011; Habib et al., 1998), as even when wastewaters are treated, treatment plants do not have a specific removal phase for MPs (Freeman et al., 2020).

4.2.2. Microplastic abundances

The lack of a standardized method for extracting and analyzing MP in environmental samples makes difficult comparisons across studies, often yielding limited information. Despite differences in the characteristics of study sites and analytical methods, comparing MP levels among locations around the world offers significant insights that broaden our understanding of global marine pollution and contextualizes the specific conditions of the area under investigation. Few published studies have employed NR staining for MP analyses in ^{210}Pb-dated sedimentary cores; hence, only results obtained without staining were compared with recent studies in coastal sediments. Indeed, the MP abundances in the sediment cores from Estero de Urías Lagoon fell within the fourth quartile (i.e., the top 25 % of values) of a database compiled from the literature of MP abundances in ^{210}Pb-dated sediment cores from diverse coastal environments worldwide (Fig. 6).

Among the most relevant human-related factors driving the level of MP contamination are high population density, mismanagement of plastic waste, proximity to urban and industrial areas (including tourism attractions, fishing grounds, maritime transportation facilities, greenhouse cultivation areas), sewage outlets and wastewater treatment plants (Hantoro et al., 2019; Wang et al., 2020; Wei et al., 2022). However, the flushing rate, i.e., the rate at which water enters, circulates through, and exits the lagoon, is also a fundamental physical property that controls the retention time and pollutant accumulation (Anthony et al., 2009). Thus, the relatively high MP abundances in EUL cores can not only be explained as a result of the various sources of pollution that converge in the lagoon (e.g., urban, industrial and port wastewater discharges) but also by the inverse estuarine circulation pattern that

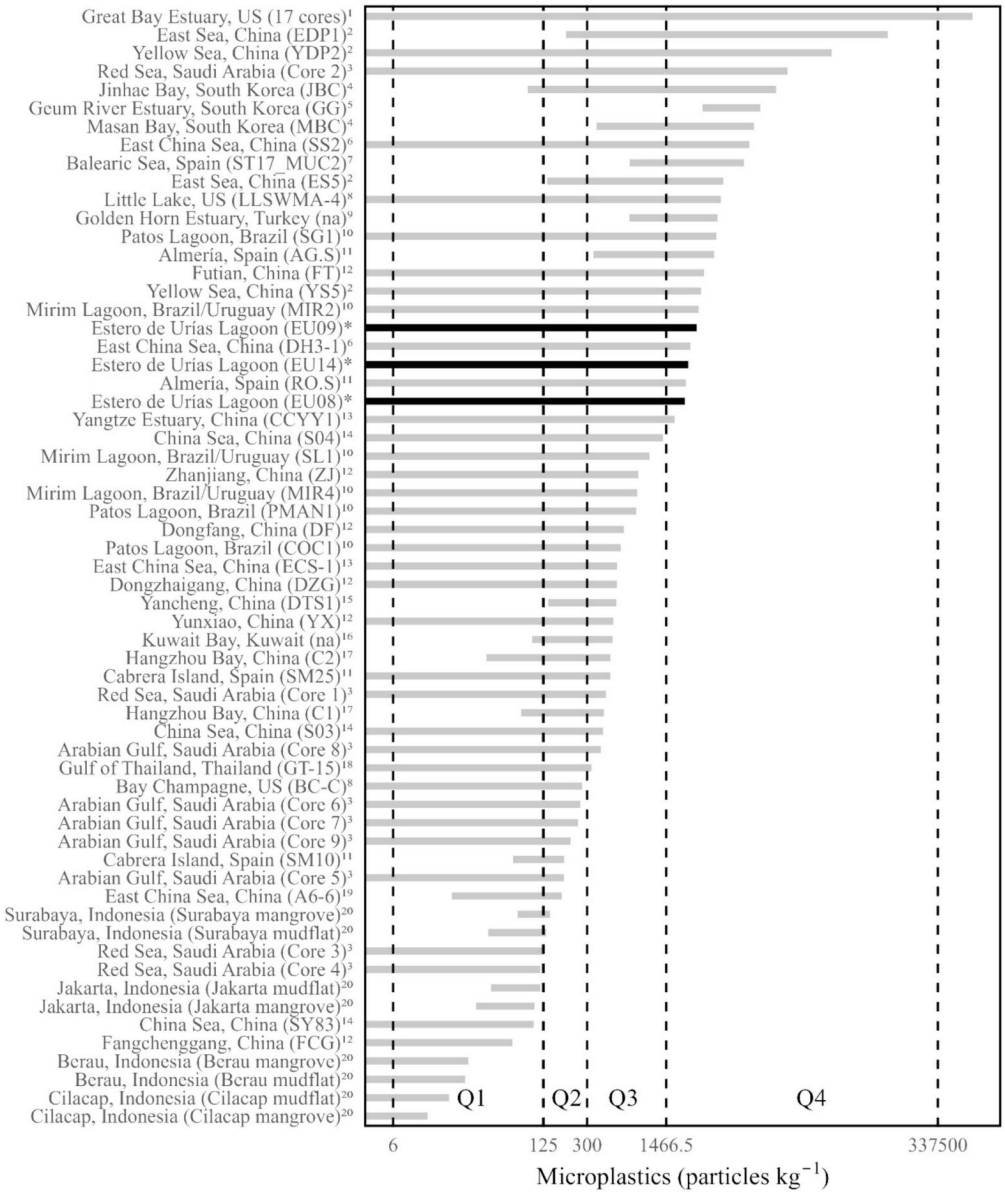

Fig. 6. Microplastic (MP) abundances in ^{210}Pb-dated sediment cores from coastal sites worldwide. Bars show MP ranges from this study (*, black) and reported in the literature (grey): Cheng et al. (2021)[1], Eo et al. (2022)[2], Martin et al. (2020)[3], Eo et al. (2023)[4], Park et al. (2023)[5]; Lin et al. (2021)[6]; Simon-Sánchez et al. (2022)[7]; Culligan et al. (2022)[8]; Belivermiş et al. (2021)[9]; Alves et al. (2023)[10]; Dahl et al. (2021)[11]; Yu et al. (2023)[12]; Chen et al. (2024)[13]; Chen et al. (2020)[14]; Zhou et al. (2024)[15]; Uddin et al. (2021)[16]; Li et al. (2020)[17]; Matsuguma et al. (2017)[18]; Wang et al. (2018)[19]; Cordova et al. (2023)[20].

characterizes it, which promotes water retention and the accumulation of pollutants, including MP (Cardoso-Mohedano et al., 2023).

The higher abundances of suspected MP in stained than in unstained filters (Fig. 2a, b) were because the use of NR solution and the fluorescence lamp improved the visual identification of particles, facilitating the identification of transparent pieces that might have otherwise gone unnoticed. Considering that sediments may accumulate high percentages of white and colorless particles (up to 95 %; Dobaradaran et al., 2018), only results from the NR-stained filters are discussed further.

The higher MP abundance in EU14 compared to the other cores was attributed to EUL's hydrodynamics, since EU14 was collected in the innermost part of the lagoon (Fig. 1), where slower currents (0.31 m s^{-1}) and longer water turnover (around 70 days) occur, making it the most vulnerable zone to contaminant accumulation (Cardoso et al., 2015). Indeed, the simulation of the transport and accumulation of polyethylene fibers released from Infiernillo Inlet (Fig. 1) indicated that, on average, particles accumulated inside EUL, mostly at the innermost area of the upper lagoon (Cardoso-Mohedano et al., 2023). Urban planning in Mazatlán City should account for the confinement of currents in the inner part of the EUL, which favors sediment and pollutant accumulation; thus, to improve the lagoon's environmental quality, where both wild and farmed fishery products are produced, discharges of treated or untreated waste should be avoided.

4.2.3. Temporal distribution of microplastic fluxes

Although MP abundances in EU14 were significantly ($p < 0.05$) higher than those in EU08 and EU09 in both periods, the MP fluxes (g cm^{-2} $year^{-1}$) were comparable among the three cores (Fig. 2). This finding i) indicates that the load of suspended MP particles is homogenized by currents before deposition (Cardoso-Mohedano et al., 2023), and ii) emphasizes the importance of comparing historical data in terms of fluxes instead of concentrations, since fluxes are normalized by the mass accumulation rates.

The acceleration of the accumulation of MP particles per unit area (i.e., the slopes of MP flux versus time) in all cores was positive in both periods (1950 to <1990 and 1990–2021), and cores EU09 and EU14 showed increments since 1990, capturing the acceleration of MP production over time (Fig. S5). This could be related to both Mazatlan City's population growth and the increasing availability of plastic products, plastic consumption, and residue wasting, leading to an increased release of raw and treated urban and industrial wastes that eventually reached EUL. Despite Mazatlán City's population growing at a similar pace since the 1950s (Fig. 2c; INEGI, 2024), the growth rate of the annual global polymer resin and fiber production, at least during the period 1990–2015, was about 3.5 higher than the growth rate during the earlier period (Fig. S5).

The acceleration of MP accumulation was higher in EU14 than in EU09 in both periods; however, EU08 had the highest value in the early period and the lowest in the most recent one (Fig. 4). The notable increase in MP flux in EU08 from 1950 to <1990 (acceleration of ~325 particles m^{-2} $year^{-2}$; Fig. 4) can be ascribed to the population growth of Mazatlán City (mainly towards the eastern part of EUL) characterized by its highest inflection during this period (Fig. 2c). Additionally, the expansion of human settlements, reflected in the development of popular neighborhoods in the 1960s (surrounding the Infiernillo Inlet) and the growth of industrial infrastructure (bordering the navigation channel of EUL), including the establishment of the Bonfil industrial park in the 1970s (Vasavilbazo Saucedo and Covantes Rodríguez, 2012), collectively contributed to an augmented discharge of wastewater into the lagoon (Sánchez Rodríguez and Calvario Martínez, 2020). On the other hand, as wastewater treatment plants and shrimp farms are known as potential sources of MP (Liu et al., 2021; Lusher et al., 2017) the increase in MP flux during the most recent period (1990–2021) in EU14 and EU09 (acceleration of ~1, 293 and ~465 particles m^{-2} $year^{-2}$, respectively; Fig. 4) is most likely due to the installation of four wastewater treatment plants (since the early 2000s) and several shrimp farms (since the late 1980s) that discharge both treated and untreated wastewater into the innermost area of EUL (Fig. 1).

4.3. Polymer identification of the suspected MP particles

PET, the synthetic polymer most frequently detected among the particles analyzed (Fig. 5), along with PE and PP, are among the top four types of polymers (PP, PE, PVC, and PET) with the highest global production (PE, 2023). They are also among the most common synthetic polymers (PE, PP, PET, and PS) reported for coastal ecosystems worldwide, as they are commonly used to manufacture everyday plastic products (Gündoğdu, 2022) and are widely used materials in the packaging and construction industries. Interestingly, PET appeared in the three sediment records since the 1970s, most likely because PET bottles came into widespread use in the mid-1970s, after Coca-Cola and Pepsi-Cola began bottling carbonated beverages (Smith, 1975).

While this study effectively reconstructed the temporal variation of MP abundances and the increasing trends in MP fluxes in EUL sediments since the mid-20th century, our results may be limited by the relatively small number of particles (~10 % of the total counts) analyzed for polymer identification, as recent recommendations suggest analyzing a larger number of particles to improve result representativeness (De Frond et al., 2023). Nevertheless, the consistency of our results across the three sediment cores analyzed in this study, as well as with our previous studies in suspended and surface sediments that used the same methodology (Cardoso-Mohedano et al., 2023; Rios-Mendoza et al., 2021) supports the reliability of our findings. Certainly, more advanced mathematical approaches to the problem of sample representativeness and uncertainty reporting are urgently needed.

The prevalence of cellulosic fibers among the particles analyzed in EUL sediments aligns with findings elsewhere, highlighting their significant role in marine MP pollution (Cashman et al., 2022). The identification of cellulose fibers might be perceived as irrelevant because they are not considered plastics and, due to the rapid degradation of natural fibers, they are thought to cause no harm to the environment; however, both fiber types sorb chemical pollutants and are vectors for chemical pollution dispersion (Ladewig et al., 2015). Although information is still scarce, it has been recently reported that both natural and synthetic microfibers impact the growth and behavior of estuarine organisms during their early life stages (Siddiqui et al., 2023). In addition, cellulose is used for many different products (e.g., paper, textiles, and cardboard) and it is also an important additive for the tobacco industry, where it is used to produce reconstituted tobacco and to prepare both cigarette paper and filter (DKFZ, 2012). Thus, cellulose fibers still represent an additional source of anthropogenic environmental contamination that must be better understood (Stanton et al., 2024).

5. Conclusions

The study aimed to assess the temporal variation of microplastics (MP) abundances and fluxes in three ^{210}Pb dated sediment cores from Estero de Urías Lagoon (EUL), an urbanized coastal lagoon at the entrance of the Gulf of California. Despite challenges posed by atypical ^{210}Pb profiles and low ^{137}Cs activities (<1.2 Bq kg^{-1}), the historical trends of MP contamination were coherent across the sediment cores, confirming the reliability of the methodology, which could be reproduced in other coastal lagoons, although we stress the need for independent markers to corroborate age models. The absence of MP before the 1950s might be useful to validate ^{210}Pb-derived age models where the ^{137}Cs signal is not detectable, and the onset of MP particles may be an additional marker of the Anthropocene epoch.

Sediments contained predominantly fibers (66–89 %) and fragments (11–34 %), mostly blue in color (38–74 %). MP abundances (200–2701 particles kg^{-1} in unstained filters) ranked among the highest in ^{210}Pb-dated marine sediments worldwide. Since EUL upholds subsistence fishing and shrimp aquaculture activities, this finding underscores the

need for immediate attention to mitigate plastic pollution impacts on aquatic life and human populations reliant on seafood.

A possible limitation of this study is the small number of particles analyzed for polymer identification; however, results were consistent across cores, showing the prevalence (14–50 %) of polyethylene terephthalate (PET) since the 1970s. Thus, reducing PET use, improving recycling rates, and raising awareness to prevent PET waste from entering the environment would be beneficial.

MP fluxes were comparable among cores, increasing from the onset of global plastic commercialization in the 1950s to the present. Accelerated MP accumulation since the 1990s (annual growth rate between 299 and 1293 particles m^{-2} $year^{-1}$, depending on the core) were influenced by the increasing plastic production, population growth, and hydrodynamics of the sampling site. The highest MP fluxes, between 1990 and 2021, at the lagoon's innermost part might result from treated and untreated wastewater discharges from wastewater treatment plants and shrimp farms. Urban planning should avoid placing known MP sources in coastal areas with low flushing rates.

The increasing MP presence in EUL highlights the growing threat of plastic contamination in coastal ecosystems, emphasizing the global need to regulated plastic production, use, and disposal, to develop efficient education strategies, and sanitation and coastal management programs to protect coastal environments and communities from incessant MP contamination.

CRediT authorship contribution statement

Ana Carolina Ruiz-Fernández: Writing – review & editing, Writing – original draft, Supervision, Resources, Project administration, Methodology, Investigation, Funding acquisition, Formal analysis, Data curation, Conceptualization. **Libia Hascibe Pérez-Bernal:** Writing – review & editing, Validation, Formal analysis. **Joan-Albert Sanchez-Cabeza:** Writing – review & editing, Supervision, Resources, Methodology, Investigation, Conceptualization. **Gladys Valencia-Castañeda:** Writing – review & editing, Supervision, Formal analysis. **Jorge Feliciano Ontiveros-Cuadras:** Writing – review & editing, Investigation, Formal analysis. **Carlos Manuel Alonso-Hernández:** Writing – review & editing, Investigation, Funding acquisition.

Declaration of competing interest

The authors declare that they have no known competing financial interests or personal relationships that could have appeared to influence the work reported in this paper.

Data availability

Data will be made available on request.

Acknowledgments

This project was supported by the grants CRP IAEA-K41019/IAEA-UNAM 23425, CRP IAEA-K41024-UNAM 26905, IAEA/TC-Regional Projects RLA7025 and RRLA7028, CONACYT 316743, and UNAM/DGAPA/PAPIIT IN109024 and IN110624. Authors are grateful for the support received from H. Bojórquez-Leyva, J.R. Rivera-Hernández, J.G. Pichardo-Velarde and J.E.Mendoza-Castañeda (laboratory assistance), B. Yáñez-Chávez (sampling work), C. Súarez-Gutiérrez (informatics) and L.F. Álvarez-Sánchez (data curation and coding). Special thanks are extended to D.L. López-Cuevas for her dedicated efforts to meet the objectives of this project and to R. Alonso Rodríguez for generously contributing expertise and laboratory resources. This work is dedicated to the memory of our captain, Sergio Rendón-Rodríguez, whose generosity and enthusiasm continue to inspire us. This is a contribution from the REMARCO network (https://remarco.org/). The IAEA is grateful to the Government of the Principality of Monaco for the support provided to its Marine Environment Laboratories.

Appendix A. Supplementary data

Supplementary data to this article can be found online at https://doi.org/10.1016/j.scitotenv.2024.175613.

References

Alcérreca-Huerta, J.C., Cruz-Ramírez, C.J., de Almeida, L.R., Chávez, V., Silva, R., 2022. Interconnections between coastal sediments, hydrodynamics, and ecosystem profiles on the Mexican Caribbean Coast. Land 11 (4), 524. https://doi.org/10.3390/land11040524.

Aldana-Gutiérrez, G., Ruiz-Fernández, A.C., Pérez-Bernal, L.H., Flores-Verdugo, F., Cuéllar-Martínez, T., Sanchez-Cabeza, J.A., 2021. Flujos e inventarios de carbono azul en manglares asociados a una laguna costera antropizada. Geofis. Int. 60 (1), 13–30. https://doi.org/10.22201/igeof.00167169p.2021.60.1.2011.

Alves, F.L., Pinheiro, L.M., Bueno, C., Agostini, V.O., Perez, L., Fernandes, E.H.L., Weschenfelder, J., Leonhardt, A., Domingues, M., Pinho, G.L.L., García-Rodríguez, F., 2023. The use of microplastics as a reliable chronological marker of the Anthropocene onset in Southeastern South America. Sci. Total Environ. 857, 159633 https://doi.org/10.1016/j.scitotenv.2022.159633.

AMC, 2016. z-Scores and other scores in chemical proficiency testing—their meanings, and some common misconceptions. Analytical Methods Committee, AMCTB No. 74 Anal. Methods 8 (28), 5553–5555. https://doi.org/10.1039/C6AY90078J.

Anthony, A., Atwood, J., August, P., Byron, C., Cobb, S., Foster, C., Fry, C., Gold, A., Hagos, K., Heffner, L., Kellogg, D.Q., Lellis-Dibble, K., Opaluch, J.J., Oviatt, C., Pfeiffer-Herbert, A., Rohr, N., Smith, L., Smythe, T., Swift, J., Vinhateiro, N., 2009. Coastal lagoons and climate change: ecological and social ramifications in U.S. Atlantic and Gulf coast ecosystems. Ecol. Soc. 14 (1), 8.

Aoyama, M., Hirose, K., Igarashi, Y., 2006. Re-construction and updating our understanding on the global weapons tests ^{137}Cs fallout. J. Environ. Monitor. 8 (4), 431. https://doi.org/10.1039/b512601k.

Athapaththu, A.M.A.I.K., Thushari, G.G.N., Dias, P.C.B., Abeygunawardena, A.P., Egodauyana, K.P.U.T., Liyanage, N.P.P., Pitawala, H.M.J.C., Senevirathna, J.D.M., 2020. Plastics in surface water of southern coastal belt of Sri Lanka (Northern Indian Ocean): distribution and characterization by FTIR. Mar. Pollut. Bull. 161, 111750 https://doi.org/10.1016/J.MARPOLBUL.2020.111750.

Barsanti, M., Garcia-Tenorio, R., Schirone, A., Rozmaric, M., Ruiz-Fernández, A.C., Sanchez-Cabeza, J.A., Delbono, I., Conte, F., De Oliveira Godoy, J.M., Heijnis, H., Yii, M.W., Osvath, I., 2020. Challenges and limitations of the ^{210}Pb sediment dating method: results from an IAEA modelling interlaboratory comparison exercise. Quat. Geochronol. 59 https://doi.org/10.1016/j.quageo.2020.101093.

Bé, M.M., Chisté, V., Dulieu, C., Browne, E., Baglin, C., Chechev, V., Kuzmenco, N., Helmer, R., Kondev, F., MacMahon, D., Lee, K.B., 2006. Monographie BIPM-5 Table of Radionuclides (Vol. 3 – A = 3 to 244) (Bureau International des Poids et Measures, Ed.). BIPM. http://www.lnhb.fr/accueil/donnees-nucleaires/donnees-nucleaires-tableau/.

Bé, M.M., Chisté, V., Dulieu, C., Browne, E., Chechev, V., Kuzmenko, K., Kondev, F., Luca, A., Galán, M., Pearce, A., Huang, X., 2008. Monographie BIPM-5 Table of Radionuclides (Vol. 4-A = 133 to 252) (Bureau International des Poids et Mesures, Ed.). http://www.lnhb.fr/accueil/donnees-nucleaires/donnees-nucleaires-tableau/.

Belivermiş, M., Kılıç, Ö., Sezer, N., Sıkdokur, E., Güngör, N.D., Altuğ, G., 2021. Microplastic inventory in sediment profile: a case study of Golden Horn Estuary, Sea of Marmara. Marine Pollution Bulletin 173, 113117. https://doi.org/10.1016/J.MARPOLBUL.2021.113117.

Browne, M.A., Crump, P., Niven, S.J., Teuten, E., Tonkin, A., Galloway, T., Thompson, R., 2011. Accumulation of microplastic on shorelines woldwide: sources and sinks. Environ. Sci. Tech. 45 (21), 9175–9179. https://doi.org/10.1021/ES201811S/ASSET/IMAGES/MEDIUM/ES-2011-01811S_0003.GIF.

Cai, H., Du, F., Li, L., Li, B., Li, J., Shi, H., 2019. A practical approach based on FT-IR spectroscopy for identification of semi-synthetic and natural celluloses in microplastic investigation. Sci. Total Environ. 669, 692–701. https://doi.org/10.1016/j.scitotenv.2019.03.124.

Cardoso-Mohedano, J.G., Bernardello, R., Sanchez-Cabeza, J.A., Molino-Minero-Re, E., Ruiz-Fernández, A.C., Cruzado, A., 2015. Accumulation of conservative substances in a sub-tropical coastal lagoon. Estuar. Coast. Shelf Sci. 164, 1–9. https://doi.org/10.1016/j.ecss.2015.06.022.

Cardoso-Mohedano, J.G., Ruiz-Fernández, A.C., Sanchez-Cabeza, J.-A., Camacho-Torres, S.M., Ontiveros-Cuadras, J.F., 2023. Microplastics transport in a low-inflow estuary at the entrance of the Gulf of California. Sci. Total Environ. 870, 161825 https://doi.org/10.1016/j.scitotenv.2023.161825.

Cashman, M.A., Langknecht, T., El Khatib, D., Burgess, R.M., Boving, T.B., Robinson, S., Ho, K.T., 2022. Quantification of microplastics in sediments from Narragansett Bay, Rhode Island USA using a novel isolation and extraction method. Mar. Pollut. Bull. 174, 113254 https://doi.org/10.1016/j.marpolbul.2021.113254.

Cearreta, A., Machain-Castillo, M.L., Ruíz-Fernández, A.C., Sánchez-Cabeza, J.-A., Serrato-De la Peña, J.L., Flores-Verdugo, F., Pérez-Bernal, L.H., 2021. Características geoquímicas y micropaleontológicas de las marismas en el Estero de Urías, Golfo de California, México. Cuaternario y Geomorfología 35 (1–2), 147–164. https://doi.org/10.17735/cyg.v35i1-2.89190.

Chen, M., Du, M., Jin, A., Chen, S., Dasgupta, S., Li, J., Xu, H., Ta, K., Peng, X., 2020. Forty-year pollution history of microplastics in the largest marginal sea of the

western Pacific. Geochemical Perspectives Letters 13, 42–47. https://doi.org/10.7185/GEOCHEMLET.2012.

Chen, B., Zhang, Z., Wang, T., Hu, H., Qin, G., Lu, T., Hong, W., Hu, J., Penuelas, J., Qian, H., 2023. Global distribution of marine microplastics and potential for biodegradation. J. Hazard. Mater. 451, 131198 https://doi.org/10.1016/j.jhazmat.2023.131198.

Chen, H., Cheng, Y., Wang, Y., Ding, Y., Wang, C., Feng, X., Fan, Q., Yuan, F., Fu, G., Gao, B., Liu, K., Zou, X., 2024. Microplastics: a potential proxy for tracing extreme flood events in estuarine environments. Sci. Total Environ. 918, 170554 https://doi.org/10.1016/J.SCITOTENV.2024.170554.

Cheng, M.L.H., Lippmann, T.C., Dijkstra, J.A., Bradt, G., Cook, S., Choi, J.G., Brown, B.L., 2021. A baseline for microplastic particle occurrence and distribution in Great Bay Estuary. Mar. Pollut. Bull. 170, 112653 https://doi.org/10.1016/J.MARPOLBUL.2021.112653.

Comnea-Stancu, I.R., Wieland, K., Ramer, G., Schwaighofer, A., Lendl, B., 2017. On the identification of rayon/viscose as a major fraction of microplastics in the marine environment: discrimination between natural and manmade cellulosic fibers using Fourier transform infrared spectroscopy. Appl. Spectrosc. 71 (5), 939–950. https://doi.org/10.1177/0003702816660725.

CONAGUA, 2022. Inventario Nacional de Plantas Municipales de Potabilización y de Tratamiento de Aguas Residuales en Operación Diciembre 2022 (Comisión Nacional del Agua, Ed.). https://files.conagua.gob.mx/conagua/publicaciones/Publicaciones/SGAPDS-8-23.pdf.

Cordova, M.R., Ulumuddin, Y.I., Lubis, A.A., Kaisupy, M.T., Wibowo, S.P.A., Subandi, R., Yogaswara, D., Purbonegoro, T., Renyaan, J., Nurdiansah, D., Sugiharto, U., Shintianata, D., Meiliastri, S.S., Andini, F.P., Suratno, Ilman, M., Anggoro, A.W., Basir, Cragg, S.M., 2023. Microplastics leaving a trace in mangrove sediments ever since they were first manufactured: a study from Indonesia mangroves. Mar. Pollut. Bull. 195, 115517 https://doi.org/10.1016/J.MARPOLBUL.2023.115517.

Culligan, N., Liu, K. Biu, Ribble, K., Ryu, J., Dietz, M., 2022. Sedimentary records of microplastic pollution from coastal Louisiana and their environmental implications. J. Coast. Conserv. 26 (1), 1–14. https://doi.org/10.1007/S11852-021-00847-Y/FIGURES/9.

Dahl, M., Bergman, S., Björk, M., Diaz-Almela, E., Granberg, M., Gullström, M., Leiva-Dueñas, C., Magnusson, K., Marco-Méndez, C., Piñeiro-Juncal, N., Mateo, M.Á., 2021. A temporal record of microplastic pollution in Mediterranean seagrass soils. Environ. Pollut. 273, 116451 https://doi.org/10.1016/J.ENVPOL.2021.116451.

Dawson, A.L., Santana, M.F.M., Nelis, J.L.D., Motti, C.A., 2023. Taking control of microplastics data: a comparison of control and blank data correction methods. J. Hazard. Mater. 443, 130218 https://doi.org/10.1016/j.jhazmat.2022.130218.

De Frond, H., O'Brien, A.M., Rochman, C.M., 2023. Representative subsampling methods for the chemical identification of microplastic particles in environmental samples. Chemosphere 310, 136772. https://doi.org/10.1016/j.chemosphere.2022.136772.

Deng, H., Wei, R., Luo, W., Hu, L., Li, B., Di, Y., Shi, H., 2020. Microplastic pollution in water and sediment in a textile industrial area. Environ. Pollut. 258, 113658 https://doi.org/10.1016/J.ENVPOL.2019.113658.

Díaz-Asencio, M., Sanchez-Cabeza, J.-A., Ruiz-Fernández, A.C., Corcho-Alvarado, J.A., Pérez-Bernal, L.H., 2020. Calibration and use of well-type germanium detectors for low-level gamma-ray spectrometry of sediments using a semi-empirical method. J. Environ. Radioact. 225, 106385 https://doi.org/10.1016/j.jenvrad.2020.106385.

DKFZ, 2012. Additives in tobacco products. Cellulose fibre. https://www.dkfz.de/de/tabakkontrolle/download/PITOC/PITOC_Tobacco_Additives_Cellulose_Fibre.pdf.

Dobaradaran, S., Schmidt, T.C., Nabipour, I., Khajeahmadi, N., Tajbakhsh, S., Saeedi, R., Javad Mohammadi, M., Keshtkar, M., Khorsand, M., Faraji Ghasemi, F., 2018. Characterization of plastic debris and association of metals with microplastics in coastline sediment along the Persian Gulf. Waste Manag. 78, 649–658. https://doi.org/10.1016/J.WASMAN.2018.06.037.

Drexler, J.Z., Fuller, C.C., Archfield, S., 2018. The approaching obsolescence of 137Cs dating of wetland soils in North America. Quat. Sci. Rev. 199, 83–96. https://doi.org/10.1016/j.quascirev.2018.08.028.

Duis, K., Coors, A., 2016. Microplastics in the aquatic and terrestrial environment: sources (with a specific focus on personal care products), fate and effects. Environ. Sci. Eur. 28 (1), 1–25. https://doi.org/10.1186/S12302-015-0069-Y.

Eo, S., Hong, S.H., Song, Y.K., Han, G.M., Seo, S., Park, Y.G., Shim, W.J., 2022. Underwater hidden microplastic hotspots: historical ocean dumping sites. Water Res. 216, 118254 https://doi.org/10.1016/J.WATRES.2022.118254.

Eo, S., Hong, S.H., Cho, Y., Song, Y.K., Han, G.M., Shim, W.J., 2023. Spatial distribution and historical trend of microplastic pollution in sediments from enclosed bays of South Korea. Mar. Pollut. Bull. 193, 115121 https://doi.org/10.1016/J.MARPOLBUL.2023.115121.

Freeman, S., Booth, A.M., Sabbah, I., Tiller, R., Dierking, J., Klun, K., Rotter, A., Ben-David, E., Javidpour, J., Angel, D.L., 2020. Between source and sea: the role of wastewater treatment in reducing marine microplastics. J. Environ. Manage. 266, 110642 https://doi.org/10.1016/J.JENVMAN.2020.110642.

Geyer, R., Jambeck, J.R., Law, K.L., 2017. Production, use, and fate of all plastics ever made. Science Advances 3 (7). https://doi.org/10.1126/SCIADV.1700782.

Gündoğdu, S., 2022. Polymer types of microplastic in coastal areas. In: Hashmi, M.Z. (Ed.), Microplastic Pollution. Emerging Contaminants and Associated Treatment Technologies. Springer, pp. 77–88. https://doi.org/10.1007/978-3-030-89220-3_4.

Habib, D., Locke, D.C., Cannone, L.J., 1998. Synthetic fibers as indicators of municipal sewage sludge, sludge products, and sewage treatment plant effluents. Water Air Soil Pollut. 103 (1–4), 1–8. https://doi.org/10.1023/A:1004908110793/METRICS.

Hantoro, I., Löhr, A.J., Van Belleghem, F.G.A.J., Widianarko, B., Ragas, A.M.J., 2019. Microplastics in coastal areas and seafood: implications for food safety. Food Additives & Contaminants: Part A 36 (5), 674–711. https://doi.org/10.1080/19440049.2019.1585581.

Heiri, O., Lotter, A.F., Lemcke, G., 2001. Loss on ignition as a method for estimating organic and carbonate content in sediments: reproducibility and comparability of results. J. Paleolimnol. 25 (1), 101–110. https://doi.org/10.1023/A:1008119611481.

Hidalgo-Ruz, V., Gutow, L., Thompson, R.C., Thiel, M., 2012. Microplastics in the marine environment: a review of the methods used for identification and quantification. Environ. Sci. Technol. 46 (6), 3060–3075. https://doi.org/10.1021/es2031505.

Horowitz, J.A., 1985. A Primer on Trace Metal Sediment Shemistry. US Geological Survey.

Hossain, M.S., Rahman, M.S., Uddin, M.N., Sharifuzzaman, S.M., Chowdhury, S.R., Sarker, S., Nawaz Chowdhury, M.S., 2020. Microplastic contamination in Penaeid shrimp from the Northern Bay of Bengal. Chemosphere 238, 124688. https://doi.org/10.1016/J.CHEMOSPHERE.2019.124688.

INEGI, 2017. Anuario estadístico y geográfico de Sinaloa 2017 (Instituto Nacional de Estadística y Geografía, Ed.). https://www.datatur.sectur.gob.mx/ITxEF_Docs/SIN_ANUARIO_PDF.pdf.

INEGI, 2024. Censo de Población y Vivienda 2020. Instituto Nacional de Estadística y Geografía. https://www.inegi.org.mx/app/cpv/2020/resultadosrapidos/default.html?texto=Mazatlan.

Karnes, H.T., March, C., 1993. Precision, accuracy, and data acceptance criteria in biopharmaceutical analysis. Pharm. Res. 10 (10), 1420–1426. https://doi.org/10.1023/A:1018958805795.

Key, S., Ryan, P.G., Gabbott, S.E., Allen, J., Abbott, A.P., 2024. Influence of colourants on environmental degradation of plastic litter. Environ. Pollut. 347, 123701 https://doi.org/10.1016/j.envpol.2024.123701.

Krishnaswamy, S., Lal, D., Martin, J.M., Meybeck, M., 1971. Geochronology of lake sediments. Earth Planet. Sci. Lett. 11 (1–5), 407–414. https://doi.org/10.1016/0012-821X(71)90202-0.

Ladewig, S.M., Bao, S., Chow, A.T., 2015. Natural fibers: a missing link to chemical pollution dispersion in aquatic environments. Environ. Sci. Technol. 49 (21), 12609–12610. https://doi.org/10.1021/acs.est.5b04754.

Li, J., Huang, W., Xu, Y., Jin, A., Zhang, D., Zhang, C., 2020. Microplastics in sediment cores as indicators of temporal trends in microplastic pollution in Andong salt marsh, Hangzhou Bay, China. Regional Studies in Marine Science 35, 101149. https://doi.org/10.1016/J.RSMA.2020.101149.

Lin, J., Xu, X.M., Yue, B.Y., Xu, X.P., Liu, J.Z., Zhu, Q., Wang, J.H., 2021. Multidecadal records of microplastic accumulation in the coastal sediments of the East China Sea. Chemosphere 270, 128658. https://doi.org/10.1016/J.CHEMOSPHERE.2020.128658.

Liu, H., Jacob, D.J., Bey, I., Yantosca, R.M., 2001. Constraints from ^{210}Pb and ^{7}Be on wet deposition and transport in a global three-dimensional chemical tracer model driven by assimilated meteorological fields. J. Geophys. Res. Atmos. 106 (D11), 12109–12128. https://doi.org/10.1029/2000JD900839.

Liu, W., Zhang, J., Liu, H., Guo, X., Zhang, X., Yao, X., Cao, Z., Zhang, T., 2021. A review of the removal of microplastics in global wastewater treatment plants: characteristics and mechanisms. Environ. Int. 146, 106277 https://doi.org/10.1016/J.ENVINT.2020.106277.

Liu, P., Liao, H., Deng, Y., Zhang, W., Zhou, Z., Sun, D., Ke, Z., Zhou, A., Tang, H., 2023. Microplastic pollution and its potential correlation with environmental factors in Daya Bay, South China Sea. Journal of Marine Science and Engineering 11 (7), 1465. https://doi.org/10.3390/jmse11071465.

Löder, M.G.J., Gerdts, G., 2015. Methodology used for the detection and identification of microplastics—a critical appraisal. In: Marine Anthropogenic Litter. Springer International Publishing, pp. 201–227. https://doi.org/10.1007/978-3-319-16510-3_8.

Lusher, A., Hollman, P., Mendoza-Hill, J., 2017. Microplastics in Fisheries and Aquaculture (Food and Agriculture Organization of the United Nations, Ed.). Food and Agriculture Organization of the United Nations. https://oceanrep.geomar.de/id/eprint/49179/1/Microplastics%20in%20fisheries%20and%20aquaculture.pdf.

Maes, T., Van der Meulen, M.D., Devriese, L.I., Leslie, H.A., Huvet, A., Frère, L., Robbens, J., Vethaak, A.D., 2017. Microplastics baseline surveys at the water surface and in sediments of the North-East Atlantic. Front. Mar. Sci. 4 https://doi.org/10.3389/fmars.2017.00135.

Marques Mendes, A., Golden, N., Bermejo, R., Morrison, L., 2021. Distribution and abundance of microplastics in coastal sediments depends on grain size and distance from sources. Mar. Pollut. Bull. 172, 112802 https://doi.org/10.1016/j.marpolbul.2021.112802.

Martin, C., Baalkhuyur, F., Valluzzi, L., Saderne, V., Cusack, M., Almahasheer, H., Krishnakumar, P.K., Rabaoui, L., Qurban, M.A., Arias-Ortiz, A., Masqué, P., Duarte, C.M., 2020. Exponential increase of plastic burial in mangrove sediments as a major plastic sink. Science Advances 6 (44). https://doi.org/10.1126/SCIADV.AAZ5593/SUPPL_FILE/AAZ5593_SM.PDF.

Martin, C., Young, C.A., Valluzzi, L., Duarte, C.M., 2022. Ocean sediments as the global sink for marine micro- and mesoplastics. Limnology and Oceanography Letters 7 (3), 235–243. https://doi.org/10.1002/lol2.10257.

Matsuguma, Y., Takada, H., Kumata, H., Kanke, H., Sakurai, S., Suzuki, T., Itoh, M., Okazaki, Y., Boonyatumanond, R., Zakaria, M.P., Weerts, S., Newman, B., 2017. Microplastics in sediment cores from Asia and Africa as indicators of temporal trends in plastic pollution. Arch. Environ. Contam. Toxicol. 73 (2), 230–239. https://doi.org/10.1007/S00244-017-0414-9/FIGURES/7.

Molino-Minero-Re, E., Cardoso-Mohedano, J.G., Ruiz-Fernández, A.C., Sanchez-Cabeza, J.-A., 2014. Comparison of artificial neural networks and harmonic analysis for sea level forecasting (Urías coastal lagoon, Mazatlán, Mexico)|Comparación de redes neuronales artificiales y análisis armónico para el pronóstico del nivel del mar (Estero de Urías, Maz.). Ciencias Marinas 40 (4), 251–261. https://doi.org/10.7773/cm.v40i4.2463.

Montaño-Ley, Y., Soto-Jiménez, M.F., Páez-Osuna, F., 2023. Seabed morphodynamics of a coastal lagoon of the Gulf of California. Environ. Fluid Mech. 23 (3), 533–549. https://doi.org/10.1007/s10652-023-09916-2.

OIEA, 2012. Radiocronología de Sedimentos Costeros Utilizando 210Pb: Modelos, Validación y Aplicaciones (Sanchez-Cabeza JA, Díaz-Asencio M, & Ruiz-Fernández AC, Eds.). Organismo Internacional de Energía Atómica. https://www.iaea.org/es/publications/8349/radiocronologia-de-sedimentos-costeros-utilizando-210pb-modelos-validacion-y-aplicaciones.

OIEA, 2021. Guía Para el Uso de Sedimentos en la Reconstrucción Histórica de la Contaminación en Zonas Costeras (Ruiz-Fernández AC & Sanchez-Cabeza JA, Eds.). https://www.iaea.org/es/publications/14762/guia-para-el-uso-de-sedimentos-en-la-reconstruccion-historica-de-la-contaminacion-en-zonas-costeras.

Ontiveros-Cuadras, J.F., Ruiz-Fernández, A.C., Pérez-Bernal, L.H., Serrato de la Peña, J. L., Sanchez-Cabeza, J.-A., 2019. Recent trace metal enrichment and sediment quality assessment in an anthropized coastal lagoon (SE Gulf of California) from 210Pb-dated sediment cores. Mar. Pollut. Bull. 149, 110653 https://doi.org/10.1016/j.marpolbul.2019.110653.

Park, J., Hong, S., Shim, W.J., Khim, J.S., Park, J., 2023. Distribution, compositional characteristics, and historical pollution records of microplastics in tidal flats of South Korea. Mar. Pollut. Bull. 189, 114741 https://doi.org/10.1016/J.MARPOLBUL.2023.114741.

PE, 2023. Plastic - The Fast Facts 2023. Plastics Europe. https://plasticseurope.org/knowledge-hub/plastics-the-fast-facts-2023/.

Pohl, F., Eggenhuisen, J.T., Kane, I.A., Clare, M.A., 2020. Transport and burial of microplastics in deep-marine sediments by turbidity currents. Environ. Sci. Technol. 54 (7), 4180–4189. https://doi.org/10.1021/acs.est.9b07527.

Rios-Mendoza, L.M., Ontiveros-Cuadras, J.F., Leon-Vargas, D., Ruiz-Fernández, A.C., Rangel-García, M., Pérez-Bernal, L.H., Sanchez-Cabeza, J.-A., 2021. Microplastic contamination and fluxes in a touristic area at the SE Gulf of California. Mar. Pollut. Bull. 170, 112638 https://doi.org/10.1016/j.marpolbul.2021.112638.

Robbins, J.A., 1978. Geochemical and geophysical applications of radioactive lead. In: Nriagu, J.O. (Ed.), *The Biochemistry of lead in the environment.* Elsevier Scientific, pp. 283–393.

Ruiz-Fernández, A.C., Hillaire-Marcel, C., 2009. ^{210}Pb-derived ages for the reconstruction of terrestrial contaminant history into the Mexican Pacific coast: potential and limitations. Mar. Pollut. Bull. 59 (4–7), 134–145. https://doi.org/10.1016/j.marpolbul.2009.05.006.

Ruiz-Fernández, A.C.C., Frignani, M., Hillaire-Marcel, C., Ghaleb, B., Arvizu, M.D.D., Raygoza-Viera, J.R.R., Páez-Osuna, F., 2009. Trace metals (Cd, Cu, Hg, and Pb) accumulation recorded in the intertidal mudflat sediments of three coastal lagoons in the Gulf of California, Mexico. Estuar. Coasts 32 (3), 551–564. https://doi.org/10.1007/s12237-009-9150-3.

Ruiz-Fernández, A.C., Sanchez-Cabeza, J.-A., Serrato de la Peña, J.L., Perez-Bernal, L.H., Cearreta, A., Flores-Verdugo, F., Machain-Castillo, M.L., Chamizo, E., García-Tenorio, R., Queralt, I., Mucciarone, D., Diaz-Asencio, M., 2016. Accretion rates in coastal wetlands of the southeastern Gulf of California and their relationship with sea-level rise. Holocene 26 (7), 1126–1137. https://doi.org/10.1177/0959683616632882.

Ruiz-Fernández, A.C., Wu, R.S.S., Lau, T.-C., Pérez-Bernal, L.H., Sánchez-Cabeza, J.A., Chiu, J.M.Y., 2018. A comparative study on metal contamination in Estero de Urias lagoon, Gulf of California, using oysters, mussels and artificial mussels: implications on pollution monitoring and public health risk. Environ. Pollut. 243, 197–205. https://doi.org/10.1016/j.envpol.2018.08.047.

Ruiz-Fernández, A.C., Alonso-Hernández, C., Espinosa, L.F., Delanoy, R., Solares Cortez, N., Lucienna, E., Castillo, A.C., Simpson, S., Pérez-Bernal, L.H., Caballero, Y., Peña-Castro, A., López-Monroy, F., Quejido-Cabezas, A.J., Garay-Tinoco, J.A., Díaz-Asencio, M., Gómez-Batista, M., Parra Lozano, J.P., Sanchez-Cabeza, J.-A., 2020. 210Pb-derived sediment accumulation rates across the Wider Caribbean Region. J. Environ. Radioact. 223–224, 106366 https://doi.org/10.1016/j.jenvrad.2020.106366.

Salazar-Pérez, C., Amezcua, F., Rosales-Valencia, A., Green, L., Pollorena-Melendrez, J. E., Sarmiento-Martínez, M.A., Tomita Ramírez, I., Gil-Manrique, B.D., Hernandez-Lozano, M.Y., Muro-Torres, V.M., Green-Ruiz, C., Piñon-Colin, T.D.J., Wakida, F.T., Barletta, M., 2021. First insight into plastics ingestion by fish in the Gulf of California, Mexico. Marine Pollution Bulletin 171, 112705. https://doi.org/10.1016/j.marpolbul.2021.112705.

Sánchez Rodríguez, M.Á., Calvario Martínez, O., 2020. Evaluación espacial y estacional del estado trófico en el sistema estuarino Urías, Mazatlán, México. Ideas En Ciencias de La Ingeniería 1 (1), 10–26. https://ideasencienciasingenieria.uaemex.mx/article/view/14588.

Sanchez-Cabeza, J.A., Ruiz-Fernández, A.C., 2012. 210Pb sediment radiochronology: an integrated formulation and classification of dating models. Geochim. Cosmochim. Acta 82, 183–200. https://doi.org/10.1016/j.gca.2010.12.024.

Sánchez-Hernández, L.J., Ramírez-Romero, P., Rodríguez-González, F., Ramos-Sánchez, V.H., Márquez Montes, R.A., Romero-Paredes Rubio, H., Sujitha, S.B., Jonathan, M.P., 2021. Seasonal evidences of microplastics in environmental matrices of a tourist dominated urban estuary in Gulf of Mexico, Mexico. Chemosphere 277, 130261. https://doi.org/10.1016/J.CHEMOSPHERE.2021.130261.

Siddiqui, S., Hutton, S.J., Dickens, J.M., Pedersen, E.I., Harper, S.L., Brander, S.M., 2023. Natural and synthetic microfibers alter growth and behavior in early life stages of estuarine organisms. Front. Mar. Sci. 9 https://doi.org/10.3389/fmars.2022.991650.

Simon-Sánchez, L., Grelaud, M., Lorenz, C., Garcia-Orellana, J., Vianello, A., Liu, F., Vollertsen, J., Ziveri, P., 2022. Can a sediment core reveal the plastic age? Microplastic preservation in a coastal sedimentary record. Environ. Sci. Tech. 56 (23), 16780–16788. https://doi.org/10.1021/ACS.EST.2C04264/ASSET/IMAGES/LARGE/ES2C04264_0005.JPEG.

Smith, G., 1975, June 4. Coca-Cola Trying a Plastic Bottle. The New York Times, p. 65. https://www.nytimes.com/1975/06/04/archives/cocacola-trying-a-plastic-bottle-pepsicola-contends-it-will.html.

Stanton, T., Johnson, M., Nathanail, P., MacNaughtan, W., Gomes, R.L., 2019. Freshwater and airborne textile fibre populations are dominated by 'natural', not microplastic, fibres. Sci. Total Environ. 666, 377–389. https://doi.org/10.1016/J.SCITOTENV.2019.02.278.

Stanton, T., James, A., Prendergast-Miller, M.T., Peirson-Smith, A., KeChi-Okafor, C., Gallidabino, M.D., Namdeo, A., Sheridan, K.J., 2024. Natural fibers: why are they still the missing thread in the textile fiber pollution story? Environ. Sci. Technol. 58 (29), 12763–12766. https://doi.org/10.1021/acs.est.4c05126.

Su, L., Sharp, S.M., Pettigrove, V.J., Craig, N.J., Nan, B., Du, F., Shi, H., 2020. Superimposed microplastic pollution in a coastal metropolis. Water Res. 168, 115140 https://doi.org/10.1016/J.WATRES.2019.115140.

Torres, F.G., De-la-Torre, G.E., 2021. Historical microplastic records in marine sediments: current progress and methodological evaluation. Reg. Stud. Mar. Sci. 46, 101868 https://doi.org/10.1016/j.rsma.2021.101868.

Turner, S., Horton, A.A., Rose, N.L., Hall, C., 2019. A temporal sediment record of microplastics in an urban lake, London, UK. Journal of Paleolimnology 61 (4), 449–462. https://doi.org/10.1007/S10933-019-00071-7/TABLES/3.

Uddin, S., Fowler, S.W., Uddin, M.F., Behbehani, M., Naji, A., 2021. A review of microplastic distribution in sediment profiles. Mar. Pollut. Bull. 163, 111973 https://doi.org/10.1016/J.MARPOLBUL.2021.111973.

Ugwu, K., Herrera, A., Gómez, M., 2021. Microplastics in marine biota: a review. Mar. Pollut. Bull. 169, 112540 https://doi.org/10.1016/J.MARPOLBUL.2021.112540.

UNSCEAR, 2000. Sources and Effects of Ionizing Radiation. UNSCEAR 2000 Report to the General Assembly, With Scientific Annexes: Vol. I. United Nations Scientific Committee on the Effects of Atomic Radiation, United Nations, p. 654.

Vasavilbazo Saucedo, A., Covantes Rodríguez, C., 2012. Construcción social de insostenibilidad en el Estero de Urías, Mazatlán, Sinaloa (Universidad Nacional Autónoma de Sinaloa, Ed.).

Verla, A.W., Enyoh, C.E., Verla, E.N., Nwarnorh, K.O., 2019. Microplastic–toxic chemical interaction: a review study on quantified levels, mechanism and implication. SN Applied Sciences 1 (11), 1400. https://doi.org/10.1007/s42452-019-1352-0.

Wang, F., Nian, X., Wang, J., Zhang, W., Peng, G., Ge, C., Dong, C., Qu, J., Li, D., 2018. Multiple dating approaches applied to the recent sediments in the Yangtze River (Changjiang) subaqueous delta. The Holocene 28 (6), 858–866. https://doi.org/10.1177/0959683617752847.

Wang, T., Hu, M., Song, L., Yu, J., Liu, R., Wang, S., Wang, Z., Sokolova, I.M., Huang, W., Wang, Y., 2020. Coastal zone use influences the spatial distribution of microplastics in Hangzhou Bay, China. Environmental Pollution 266, 115137. https://doi.org/10.1016/j.envpol.2020.115137.

Weber, C.J., Lechthaler, S., 2021. Plastics as a stratigraphic marker in fluvial deposits. Anthropocene 36, 100314. https://doi.org/10.1016/j.ancene.2021.100314.

Wei, Y., Ma, W., Xu, Q., Sun, C., Wang, X., Gao, F., 2022. Microplastic distribution and influence factor analysis of seawater and surface sediments in a typical bay with diverse functional areas: a case study in Xincun Lagoon, China. Frontiers in Environmental Science 10. https://doi.org/10.3389/fenvs.2022.829942.

Yu, L., Li, R., Chai, M., Li, B., 2023. Vertical distribution, accumulation, and characteristics of microplastics in mangrove sediment in China. Sci. Total Environ. 856, 159256 https://doi.org/10.1016/J.SCITOTENV.2022.159256.

Zhang, Y., Kang, S., Allen, S., Allen, D., Gao, T., Sillanpää, M., 2020. Atmospheric microplastics: A review on current status and perspectives. Earth Sci. Rev. 203, 103118 https://doi.org/10.1016/J.EARSCIREV.2020.103118.

Zhao, X., Wang, J., Yee Leung, K.M., Wu, F., 2022. Color: an important but overlooked factor for plastic photoaging and microplastic formation. Environ. Sci. Technol. 56 (13), 9161–9163. https://doi.org/10.1021/acs.est.2c02402.

Zhou, Y., Zhou, S., Chen, S.S., Li, Y., Chen, L., Zhang, Q., Su, B., Wang, T., 2024. Sedimentary record of microplastics in coastal wetland, eastern China. Water Res. 249, 120975 https://doi.org/10.1016/J.WATRES.2023.120975.